Higher-Order Septin Assembly Is Driven by GTP-Promoted Conformational Changes: Evidence From Unbiased Mutational Analysis in *Saccharomyces cerevisiae*

Andrew D. Weems,* Courtney R. Johnson,* Juan Lucas Argueso,† and Michael A. McMurray*,[1]
*Department of Cell and Developmental Biology, University of Colorado Anschutz Medical Campus, Aurora, Colorado 80045, and
†Department of Environmental and Radiological Health Sciences, Colorado State University, Fort Collins, Colorado 80523

ABSTRACT Septin proteins bind GTP and heterooligomerize into filaments with conserved functions across a wide range of eukaryotes. Most septins hydrolyze GTP, altering the oligomerization interfaces; yet mutations designed to abolish nucleotide binding or hydrolysis by yeast septins perturb function only at high temperatures. Here, we apply an unbiased mutational approach to this problem. Mutations causing defects at high temperature mapped exclusively to the oligomerization interface encompassing the GTP-binding pocket, or to the pocket itself. Strikingly, cold-sensitive defects arise when certain of these same mutations are coexpressed with a wild-type allele, suggestive of a novel mode of dominance involving incompatibility between mutant and wild-type molecules at the septin–septin interfaces that mediate filament polymerization. A different cold-sensitive mutant harbors a substitution in an unstudied but highly conserved region of the septin Cdc12. A homologous domain in the small GTPase Ran allosterically regulates GTP-binding domain conformations, pointing to a possible new functional domain in some septins. Finally, we identify a mutation in septin Cdc3 that restores the high-temperature assembly competence of a mutant allele of septin Cdc10, likely by adopting a conformation more compatible with nucleotide-free Cdc10. Taken together, our findings demonstrate that GTP binding and hydrolysis promote, but are not required for, one-time events—presumably oligomerization-associated conformational changes—during assembly of the building blocks of septin filaments. Restrictive temperatures impose conformational constraints on mutant septin proteins, preventing new assembly and in certain cases destabilizing existing assemblies. These insights from yeast relate directly to disease-causing mutations in human septins.

HETEROOLIGOMERIC septin assemblies control cytokinesis, microtubule-based vesicular transport, ciliogenesis, bacterial entry into host cells during infection, phagocytosis, chromosome alignment, and formation of spines in dendrites and collateral branches in axons, among other cellular processes (Hu *et al.* 2012; Mostowy and Cossart 2012; Ghossoub *et al.* 2013). In most of these cases, heterohexameric or -octameric septin complexes appear to polymerize into filaments capable of lateral "bundling" associations, frequently appearing as plasma-membrane-associated rings. Filamentous septin assemblies act as scaffolds and membrane diffusion barriers to modify membrane properties and restrict in space and time the localization of other proteins (Oh and Bi 2011).

In many organisms, distinct isoforms of particular septin subunits are expressed in a cell-type-specific manner and are often coexpressed in a given cell type. Isoforms occupy the same position within the heterooligomer and may be products of distinct genes or variants of a single gene diversified by alternative splicing or other mechanisms. Specific isoforms are able to target septin heterooligomers to specific cellular functions (García *et al.* 2011; Kim *et al.* 2011; Sellin *et al.* 2012), presumably by tailoring the structural properties of higher-order septin assemblies to the task at hand, and/or modifying the repertoire of nonseptin proteins

doi: 10.1534/genetics.114.161182
Manuscript received November 18, 2013; accepted for publication January 3, 2014; published Early Online January 7, 2014.
Available freely online through the author-supported open access option.
Supporting information is available online at http://www.genetics.org/lookup/suppl/doi:10.1534/genetics.114.161182/-/DC1.
[1]Corresponding author: Department of Cell and Developmental Biology, University of Colorado Anschutz Medical Campus, 12801 E. 17th Ave., MS 8108, Aurora, CO 80045. E-mail: michael.mcmurray@ucdenver.edu

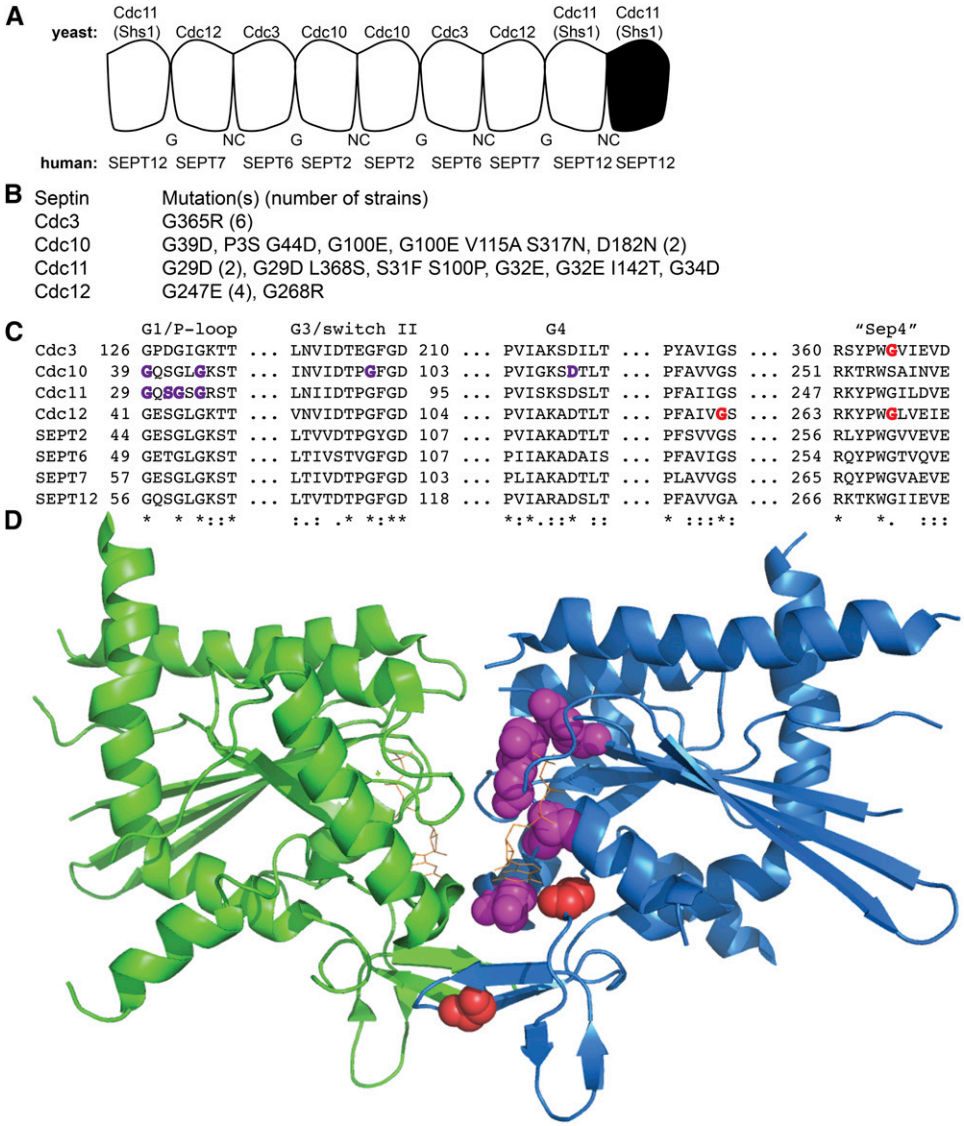

Figure 1 Heat-sensitive septin mutants substitute residues that contact bound nucleotide or the G dimerization partner. (A) Cartoon model illustrating the organization of mitotic yeast septin subunits within the septin heterooctamer, and the interfaces between them. The filled subunit represents the terminal subunit of another heterooctamer in the context of a filament. Below are identified the positions within heterooligomers predicted to be occupied by the human septins whose sequences are shown in C. (B) The substitutions found in the 24 Ts$^-$ mutant strains. When >1 strain harbored the same mutation, the number of such strains is indicated in parentheses. (C) ClustalW2 alignment of sequences surrounding the conserved motifs in yeast Cdc3, Cdc10, Cdc11, and Cdc12 and human SEPT2, SEPT6, SEPT7, and SEPT12. Colored residues are sites of substitutions: red, Cdc3 or Cdc12; purple, Cdc10 or Cdc11. Above the top sequence are labels of key GTPase motifs and other conserved features. Conservation is indicated below the alignment by the following symbols: "*," positions with a single, fully conserved residue; ":," conservation between groups of strongly similar properties; and "." conservation between groups of weakly similar properties. (D) The structure of a homodimer of the human SEPT2 bound to the nonhydrolyzable GTP analog GppNHp (PDB 3FTQ) with the residues corresponding to those found in Ts$^-$ yeast rendered as spheres and color coded as in C. GppNHp is shown in orange.

and other factors (*e.g.*, membrane lipids) with which the heterooligomers interact. In particular, the "terminal" subunit of septin heterooctamers, which mediates the ability of heterooctamers to polymerize into filaments, appears to be a common site of diversification (see the example of Shs1 in Figure 1A). Indeed, mutations in the terminal subunits are associated with human disease: SEPT9 in hereditary neuralgic amyotrophy (Kuhlenbäumer *et al.* 2005) and SEPT12 in male infertility (Kuo *et al.* 2012).

All septins studied to date bind GTP, but only some hydrolyze GTP to GDP, and significant rates of nucleotide exchange have not been observed for native septin heterooligomers (Vrabioiu *et al.* 2004; Farkasovsky *et al.* 2005). Indeed, within heterooligomers/filaments, the GTP-binding pockets are largely inaccessible to solvent, as a major oligomerization interface (called the "G interface") buries the pockets (see Figure 1) and precludes hydrolysis/exchange-mediated dynamics that are observed in other cytoskeletal polymer systems. Nonetheless, GTP binding and hydrolysis clearly play important roles in the assembly of septin heterooligomers. As in other Ras-like small GTPases, conformational changes in the "switch" regions of septins accompany GTP hydrolysis (Sirajuddin *et al.* 2009). Rather than altering interactions with "effector" proteins, however, these changes appear to modify interactions with other septins across the G interface (Sirajuddin *et al.* 2009). GTP hydrolysis also alters the conformation of the "NC" interface by which G dimers associate with other G dimers to form rod-shaped "protofilaments" (Sirajuddin *et al.* 2009), suggestive of allosteric effects that could couple the nucleotide status in the pocket of one septin to interactions between other septins. Importantly, in each case of human infertility caused by septin mutation, the mutation affected a residue predicted to contact bound nucleotide and either blocked GTP binding or hydrolysis, leading to the complete failure to assemble a filamentous septin ring called the annulus (Kuo *et al.* 2012).

Septin-encoding genes were first identified in an unbiased chemical mutagenesis screen for temperature-sensitive (Ts$^-$)

yeast strains (Hartwell 1971). At high temperature, cells carrying mutant alleles of one of only four genes—*CDC3*, *CDC10*, *CDC11*, and *CDC12*—lack an array of filaments at the mother–bud neck (Longtine *et al.* 1996) that are thought to be composed of the septins themselves (Oh and Bi 2011). The amino acid changes in seven Ts⁻ septin mutants isolated in unbiased screens have been identified: *cdc10-1* (D182N) (McMurray *et al.* 2011b), *cdc10-11* (G179D) (Cid *et al.* 1998), *cdc11-1* and *cdc11-7* (G29D) (Nagaraj *et al.* 2008), *cdc11-6* (G32E) (Nagaraj *et al.* 2008), *cdc12-1* (G247E) (Casamayor and Snyder 2003), and *cdc12-6* (L391N E392STOP) (Nagaraj *et al.* 2008). Six of these substitutions affect residues that are predicted—based on homology and using the atomic structures of human septins (Sirajuddin *et al.* 2007; 2009; Macedo *et al.* 2013)—to lie within the GTP-binding pocket, either near or in direct contact with bound nucleotide. By contrast, *cdc12-6* encodes a C-terminally truncated protein with a single substitution far from the pocket, eliminating a portion of a predicted coiled-coil-forming domain that is not conserved among all septins (Pan *et al.* 2007). Analysis of the effect of high cultivation temperature on the septin-ring-forming ability of mutant cells suggested a functional distinction between the GTP-binding-pocket mutants and the coiled-coil mutant: the pocket mutants were reportedly able to maintain a septin ring at high temperature, provided the ring had assembled at low temperature, whereas in coiled-coil-mutant cells even preformed rings disappeared at high temperature (Dobbelaere *et al.* 2003; Nagaraj *et al.* 2008). The steady-state levels of both types of mutant proteins are indistinguishable from wild type at any temperature (Nagaraj *et al.* 2008), and defects in the behavior of the pocket-mutant proteins can be detected even at permissive growth temperatures [as reduced incorporation of the mutant protein in heteromeric septin complexes (Nagaraj *et al.* 2008), and synthetic genetic phenotypes when combined with mutations in other genes (Longtine *et al.* 1996; Nagaraj *et al.* 2008)]. These findings suggested that the effect of temperature is not on the ability of the pocket-mutant proteins to bind nucleotide or to escape destruction. Instead, high temperature appeared to prevent pocket-mutant cells from assembling new septin complexes that were competent to form a filamentous ring, pointing to a structural role for GTP binding in septin–septin interactions (Nagaraj *et al.* 2008). Somewhat paradoxically, however, rings formed from complexes containing pocket-mutant proteins were thermostable, suggesting that any structural role of nucleotide is dispensable once the ring form is achieved. In coiled-coil-mutant (*cdc12-6*) cells, on the other hand, either the complexes themselves or their ability to polymerize into cortical filaments is fundamentally thermolabile.

As an unbiased approach to learn more about the requirements for yeast septin ring assembly and stability, we identified the amino acid changes in septin proteins responsible for the temperature sensitivity of an additional 25 Ts⁻ yeast strains and five cold-sensitive (Cs⁻) strains. The locations of the affected residues and our characterization of ring defects in mutant cells identify septin dimerization at the G interface—rather than GTP binding *per se*—as a critical step in ring assembly. Our data suggest a novel mechanism of quality control of septin ring formation and point to an inability to acquire functional conformations as the primary effect of temperature in Ts⁻ and Cs⁻ septin mutants.

Materials and Methods

Strains, media, and genetic manipulations

All yeast strains are listed in Table 1 and were manipulated using standard techniques (Lundblad and Struhl 2001). Yeast cells were cultivated in liquid or on solid agar plates of rich (YPD, 1% yeast extract, 2% tryptone or peptone, 2% dextrose) or synthetic (Drop Out Mix Minus various ingredients, United States Biological) media, as appropriate to maintain plasmid selection. G-418 (Geneticin) was added to YPD to a final 200 μg/ml of the active drug. Hydroxyurea (HU) was dissolved in YPD at 0.2 M. Sporulation was induced in 1% potassium acetate, 0.05% glucose, 20 mg/liter leucine, 40 mg/liter uracil. Bacterial strains DH5alpha and XL1-Blue (Agilent) were used to propagate plasmids (Table 2), of which DNA was obtained as for yeast DNA (see below) but without glass bead lysis. Yeast transformation was performed using the Frozen-EZ Yeast Transformation Kit II (Zymo Research).

Preparation of yeast DNA, PCR, cloning, PFGE, and Array-Based Comparative Genomic Hybridization

For PCR, genomic or plasmid DNA from yeast was isolated by resuspending cells in 250 μl P1 (50 mM Tris-HCl pH 8.0, 10 mM EDTA, 100 μg/ml RNase A), adding 0.5-mm glass beads to displace an additional ~250 μl of volume and vortexing for 3 min prior to addition of P2 (200 mM NaOH, 1% SDS) and N3 (4.2 M Guanidinium-HCl, 0.9 M potassium acetate, pH 4.8). Lysates were clarified by centrifugation and applied to Zyppy plasmid DNA miniprep columns (Zymo Research); then DNA was washed and eluted according to the manufacturer's instructions. Plasmids were transformed to competent bacterial cells using the Mix & Go E. coli Transformation Kit (Zymo Research) or supercompetent XL1-Blue cells according to the manufacturer's instructions. PCR was performed with various high-fidelity enzymes, typically Q5 (New England Biolabs), according to the manufacturer's instructions. Primers and nucleotides were eliminated prior to dideoxy sequencing by treatment of the PCR reaction with *Exo*I and FastAP (Fermentas), according to the manufacturer's instructions. For those PCR products that were TOPO® cloned, pCR4Blunt-TOPO® (Life Technologies) was used according to the manufacturer's instructions. PFGE and array-based comparative genomic hybridization (array-CGH), along with yeast DNA preparation for those techniques, were performed as described previously (Argueso *et al.* 2008).

Table 1 Yeast strains used in this study and the phenotypes of septin mutations

Strain	Relevant genotype[a]	Temperature-sensitive phenotype(s)[b]	Septin region affected; predicted nucleotide state[c]	Source/reference
LH10004	A364A "*cdc3-3*" ***cdc3(G365R)***	Recessive Ts$^-$ growth	"WG" motif of G interface; GTP	Hartwell (1971)
JPT2	S288C "*cdc3-6*" ***cdc3(G365R)***	Recessive Ts$^-$ growth	"WG" motif of G interface; GTP	Adams and Pringle (1984)
JPTA1506	S288C ***cdc3(G365R)***	Recessive Ts$^-$ growth	"WG" motif of G interface; GTP	J. Pringle
JPTA1509	S288C ***cdc3(G365R)***	Recessive Ts$^-$ growth	"WG" motif of G interface; GTP	J. Pringle
CBY04956	BY4741 "*cdc3-1*" ***cdc3(G365R)***::*kanMX*	Recessive slow growth at low temps, Ts$^-$ growth	"WG" motif of G interface; GTP	Li *et al.* (2011)
CBY07236	BY4741 "*cdc3-3*" ***cdc3(G365R)***::*kanMX*	Recessive Ts$^-$ growth, ring assembly (pLP29)	"WG" motif of G interface; GTP	Li *et al.* (2011)
CBY06417	BY4741 "*cdc10-1*" ***cdc10(D182N)***::*kanMX*	Recessive Ts$^-$ growth, ring stability (pLP29)	G4 motif; empty	Li *et al.* (2011)
CBY06420	BY4741 "*cdc10-2*" ***cdc10(G100E)***::*kanMX*	Recessive Ts$^-$ growth, ring stability (pML43)	G3 motif; unknown	Li *et al.* (2011)
LH310-2	A364A "*cdc10-3*" ***cdc10(G39D)***	Recessive Ts$^-$ growth	P-loop; guanosine?	Hartwell (1971)
CBY06421	BY4741 "*cdc10-4*" ***cdc10(G100E*** *V115A S317N)*::*kanMX*	Recessive Ts$^-$ growth	G3 motif; unknown	Li *et al.* (2011)
CBY06424	BY4741 "*cdc10-5*" ***cdc10***(*P3S* ***G44D***)::*kanMX*	Recessive Ts$^-$ growth, ring stability (pML43)	P-loop; guanosine?	Li *et al.* (2011)
JPT193	S288C ***cdc10(D182N)***	Recessive Ts$^-$ growth	G4 motif; empty	J. Pringle
VCY1	*leu2-3,112 trp1-1 ura3-52 his4 "cdc10-11"* ***cdc10(G179D)***	Recessive Ts$^-$ growth, ring stability (pML43)	G4 motif; empty?	Cid *et al.* (1998)
CBY08756	BY4741 "*cdc11-1*" ***cdc11(G32E*** *I142T)*::*kanMX*	Recessive Ts$^-$ growth	P-loop; guanosine?	Li *et al.* (2011)
CBY06426	BY4741 "*cdc11-2*" ***cdc11(G29D*** *L368S)*::*kanMX*	Recessive Ts$^-$ growth	P-loop; guanosine?	Li *et al.* (2011)
CBY06427	BY4741 "*cdc11-3*" ***cdc11(G29D)***::*kanMX*	Recessive Ts$^-$ growth, ring assembly (pLP29)	P-loop; guanosine?	Li *et al.* (2011)
CBY06525	BY4741 "*cdc11-4*" ***cdc11(S31F*** *S100P)*::*kanMX*	Recessive Ts$^-$ growth	P-loop; guanosine?	Li *et al.* (2011)
CBY06430	BY4741 "*cdc11-5*" ***cdc11(G34D)***::*kanMX*	Recessive Ts$^-$ growth, ring assembly (pLP17)	P-loop; guanosine?	Li *et al.* (2011)
JPT194	S288C "*cdc11-6*" ***cdc11(G32E)***	Recessive Ts$^-$ growth	P-loop; guanosine?	Adams and Pringle (1984)
JPT9	S288C "*cdc11-7*" ***cdc11(G29D)***	Recessive Ts$^-$ growth	P-loop; guanosine?	J. Pringle
C17.01D	S288C ***cdc11(G29D)***/*CDC11*	Dominant Cs$^-$ growth	P-loop; guanosine?	Moir *et al.* (1982)
N84.06D	S288C ***cdc11(G29D)***/*CDC11*	Dominant Cs$^-$ growth	P-loop; guanosine?	Moir *et al.* (1982)
P44.08C	S288C ***cdc11(G32E)***/*CDC11*	Dominant Cs$^-$ growth	P-loop; guanosine?	Moir *et al.* (1982)
Q26.15D	S288C ***cdc11(G32E)***/*CDC11*	Dominant Cs$^-$ growth	P-loop; guanosine?	Moir *et al.* (1982)
K3534	MATa *ade2-1 ade3 trp1-1 can1-100 leu2-3,112 ura3 cln1*::*hisG cln2*Δ [YCp*URA3 ADE3* P_{ADH}::*CLN2*] *"cla10-3" bud4*	Normal growth	Promoter?; GDP	Cvrcková *et al.* (1995)
K3535	MATa *ade2-1 ade3 trp1-1 can1-100 leu2-3,112 ura3 cln1*::*hisG cln2*Δ [YCp*URA3 ADE3* P_{ADH}::*CLN2*] *"cla10-1" bud4* ***cdc12(R363K)***	Cs$^-$ growth	Ran-like C-terminal extension; GDP	Cvrcková *et al.* (1995)
K3536	MATa *ade2-1 ade3 trp1-1 can1-100 leu2-3,112 ura3 cln1*::*hisG cln2*Δ [YCp*URA3 ADE3* P_{ADH}::*CLN2*] *"cla10-4" bud4*	Normal growth	Promoter?; GDP	Cvrcková *et al.* (1995)
K3538	MATa *ade2-1 ade3 trp1-1 can1-100 leu2-3,112 ura3 cln1*::*hisG cln2*Δ [YCp*URA3 ADE3* P_{ADH}::*CLN2*] *"cla10-2" bud4* ***cdc12(G247E)***/*CDC12*	Dominant Ts$^-$, Cs$^-$ growth	Nucleotide binding pocket; CTP	Cvrcková *et al.* (1995)

(continued)

Table 1, *continued*

Strain	Relevant genotype[a]	Temperature-sensitive phenotype(s)[b]	Septin region affected; predicted nucleotide state[c]	Source/reference
CBY05110	BY4741 "*cdc12-1*" ***cdc12(G247E)***::*kanMX*	Recessive Ts$^-$ growth, dominant Ts$^-$ morphology, ring assembly (pML43)	Nucleotide binding pocket; CTP	Li *et al.* (2011)
CBY05569	BY4741 "*cdc12-td*" ***Arg-DHFR^{ts}-CDC12***::*kanMX*	Recessive Ts$^-$ growth, ring stability (pML43)	N-terminal fusion to temperature-sensitive degron; GDP	Li *et al.* (2011)
JPT116	S288C ***cdc12(G247E)***	Ts$^-$ growth	Nucleotide binding pocket; CTP	J. Pringle
JPTA1435	S288C ***cdc12(G268R)***	Ts$^-$ growth	"WG" motif of G interface; GDP	J. Pringle
JPTR122	S288C ***cdc12(G247E)***	Ts$^-$ growth	Nucleotide binding pocket; CTP	J. Pringle
JPTR123	S288C ***cdc12(G247E)***	Ts$^-$ growth	Nucleotide binding pocket; CTP	J. Pringle
BY4741	*MAT**a** his3Δ1 leu2Δ0 ura3Δ0 met15Δ0*	Normal growth	N/A; N/A	Brachmann *et al.* (1998)
BY4742	*MATα his3Δ1 leu2Δ0 ura3Δ0 lys2Δ0*	Normal growth	N/A; N/A	Brachmann *et al.* (1998)
BY4743	*MAT**a**/α his3Δ1/his3Δ1 leu2Δ0/leu2Δ0 ura3Δ0/ura3Δ0 met15Δ0/MET15 lys2Δ0/LYS2*	Normal growth	N/A; N/A	Brachmann *et al.* (1998)
JTY4024	BY4742 ***shs1***Δ::*kanMX*	Cs$^-$ morphology	Protein absent	Winzeler *et al.* (1999)
MMY0104	BY4742 *ho*Δ::*kanMX*	Normal growth	N/A; N/A	Winzeler *et al.* (1999)
MMY0127[d]	***shs1***Δ::*kanMX* ***cdc11(G34D)***::*kanMX* [pML111]	Ts$^-$ growth, ring stability (pML111)	Shs1: absent. Cdc11: P-loop; guanosine?	This study
MMY0110[e]	JPT193 ***cdc3(D210G)***	Normal growth	Cdc10: G4 motif; empty. Cdc3: switch II, GTP	This study
MMY0128[f]	***cdc10(D182N)***	Ts$^-$ growth	G4 motif; empty	This study
MMY0129[f]	*CDC10 CDC3*	Normal growth	N/A; N/A	This study
MMY0130[f]	***cdc3(D210G) cdc10(D182N)***	Normal growth	Cdc10: G4 motif; empty. Cdc3: switch II, GTP	This study
MMY013[f]	***cdc3(D210G)***	Slow growth at all temps	Switch II, GTP	This study

[a] Septin mutations presumed to be responsible for the temperature-sensitive phenotype(s) are shown in boldface type.
[b] Where the distinction between failure to assemble ("ring assembly") or failure to maintain ("ring stability") a septin ring at high temperature has been made experimentally, the fluorescently tagged septin plasmid used is given in parentheses.
[c] N/A, not applicable. "?" indicates speculation without supporting evidence.
[d] Spore from cross of diploid strain made by mating JTY4024 and CBY06430 and introducing pML111 by transformation.
[e] Spontaneous suppressor of Ts$^-$ phenotype of strain JPT193.
[f] Spore from cross of MMY0100 with MMY0104. Genotypes at *MAT*, *ho*, and marker genes are unknown.

Table 2 Plasmids used in this work

Plasmid	Relevant properties	Source/reference
pCdc10-1-GFP	*CEN URA3 cdc10(D182N)-GFP*	McMurray *et al.* (2011b)
pFA6a-KanMX4	*kanMX4*	Wach *et al.* (1998)
pML43	*CEN LEU2 his3MX CDC11-YFP*	Nagaraj *et al.* (2008)
pML111	*CEN LEU2 his3MX CDC10-YFP*	Nagaraj *et al.* (2008)
pSB1	*CEN URA3 CDC11*	Versele *et al.* (2004)
pLP17	*CEN LEU2 CDC12-GFP*	Lippincott and Li (1998)
pLP29	*CEN HIS3 CDC12-GFP*	Lippincott and Li (1998)
pCR4Blunt-TOPO®	Topoisomerase-coupled cloning vector	Life Technologies
pTOPO-JPT116[a]	pCR4Blunt-TOPO *cdc12(G247E)*	This work
pTOPO-JPTR122[a]	pCR4Blunt-TOPO *cdc12(G247E)*	This work
pTOPO-JPTR123[a]	pCR4Blunt-TOPO *cdc12(G247E)*	This work
YCpK-Cdc10-1-GFP[b]	*CEN kanMX cdc10-1-GFP*	This work

[a] A central portion of the *CDC12* coding sequence from strains JPT116, JPTR122, or JPTR123 was amplified with PFU and cloned into pCR4Blunt-TOPO®.

[b] pCdc10-1-GFP was cotransformed into strain BY4742 with a PCR product amplified from template pFA6a-KanMX4 that contained the *kanMX4* cassette flanked by sequences targeting it for replacement via homologous recombination of the *URA3* marker in pCdc10-1-GFP.

Microscopy

All images were captured with an EVOSfl (Advanced Microscopy Group) all-in-one microscope equipped with an Olympus 60× oil immersion objective and GFP, YFP, and DAPI filters. For assembly-*vs.*-stability experiments, yeast cells were grown to mid-log phase at room temperature in small selective liquid cultures and then divided in half, pelleted, and resuspended in 100 μl YPD or 100 μl YPD + HU. Cultures were transferred to thin-wall PCR tubes and incubated in a thermal cycler with the following program: 4 hr at 23°, 2 hr at 37°, and hold at 4°. Cells were then transferred to water, spotted on agarose pads, and visualized by microscopy with the GFP or YFP filter, as appropriate, and 60- or 250-msec exposures at 100% intensity. Imaging of Cdc10 (D182N)-GFP was performed in a similar way with cells from a mid-log YPD + G418 culture. For DAPI staining, cells were pelleted, resuspended in 1 ml 70% ethanol for 5 min, then pelleted, washed three times with water, and resuspended in 1 ml of 0.5 μg/ml DAPI before a 1-hr incubation in the dark. DAPI-stained nuclei were visualized with the DAPI filter using a 60-msec exposure at 100% intensity.

Results

We collected Ts$^-$ mutants that were identified in chemical mutagenesis screens and determined by linkage and/or complementation to carry septin mutations (Table 1). These included six *cdc3*, six *cdc10*, seven *cdc11* (for *cdc11-1*, we obtained a different result than previously published; Nagaraj *et al.* 2008), and five *cdc12* mutants (Figure 1B). Alleles of *CDC11* had also been found in similar screens for cold-sensitive (Cs$^-$) mutants (Moir *et al.* 1982; Healy *et al.* 1991), so we analyzed four of these. Finally, as intended negative controls, we obtained four *cla10* mutants derived from a temperature-independent screen for mutants that are synthetically lethal with depletion of G1 cyclins (Cvrcková and Nasmyth 1993) and were determined by complementation to be alleles of *CDC12* (Cvrcková *et al.* 1995). However, we found that one of these, *cla10-2*, is moderately Ts$^-$ and Cs$^-$, and another, *cla10-1*, is strongly Cs$^-$ (Supporting Information, Figure S1A). From each strain, we amplified the majority of the septin ORF by PCR and either sequenced it directly or first cloned it into a plasmid and then sequenced using standard dideoxy Sanger methods.

Septin mutations that affect temperature-sensitive growth cluster around the G dimerization interface

Without exception, the affected residues in the Ts$^-$ strains lie within the dimerization interface encompassing the GTP-binding pocket (the G interface), based on the locations of the equivalent (and highly conserved) residues in human septins (Figure 1). Note that in a few instances mutations outside the G interface were identified, but in each such case a G interface substitution was also present in the same strain (Figure 1B, Table 1), and hence is likely the causative lesion. By contrast, we found no mutation in the GTP-binding pocket or G interface of any of the three Ts$^+$ *cla10* strains.

In the two *cla10* strains that grew normally at all temperatures (K3534 and K3536), we found no *CDC12* mutation in the coding region. We suspected that mutations outside the coding region could affect the amount or stability of Cdc12 transcript and reduce the amount of wild-type Cdc12 protein below a threshold required for cells to be able to tolerate G1 cyclin depletion, but above a threshold required for septin functions in morphogenesis and cytokinesis. Evidence in support of this idea came from comparison of steady-state Cdc12 levels in the four *cla10* strains: the amount of Cdc12 in K3534 (*cla10-3*) and K3536 (*cla10-4*) was appreciably lower than in the other two strains (Figure S1B).

Cold-sensitive cdc11 mutants harbor two alleles, one wild-type and one mutant allele that alone makes cells heat sensitive

Our analysis of the four Cs$^-$ *cdc11* mutants generated surprising results. In each, one or more positions in *CDC11* appeared as "mixed" peaks with two distinct nucleotides

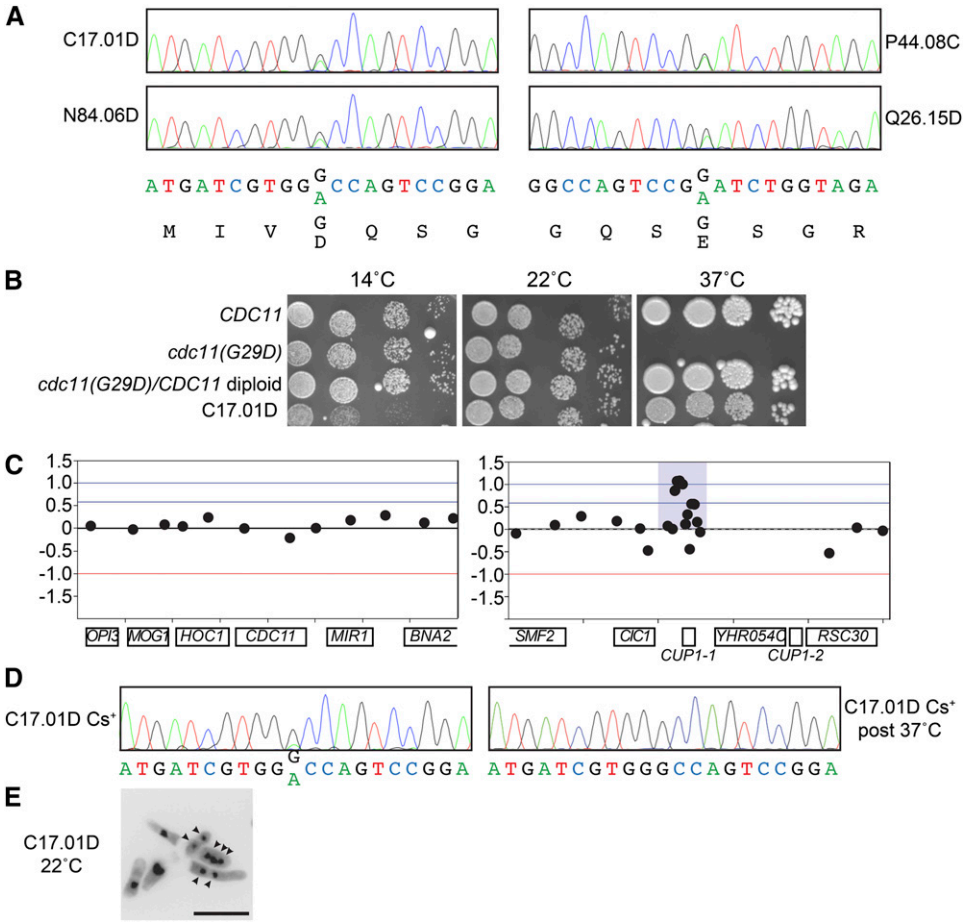

Figure 2 Cold-sensitive *cdc11* mutants have two alleles of *CDC11* and behave as semistable heterokaryons. (A) Dideoxy sequencing chromatograms demonstrating the presence of two nucleotides at a single position in PCR products of portions of the *CDC11* coding region amplified from genomic DNA of the indicated strains. Predicted amino acid changes are shown beneath each pair of images. (B) Fivefold dilution series of cells of the indicated genotypes or strain names spotted on rich (YPD) agar plates and incubated at different temperatures for the indicated number of days. Strains were: *CDC11*, BY4741; *cdc11(G29D)*, CBY06427; *cdc11(G29D)/CDC11* diploid (diploid formed by mating BY4742 with CBY06427); and the cold-sensitive *cdc11* strain C17.01D. (C) Array-CGH results for genomic regions of interest in C17.01D relative to a control haploid strain, BY4741. Each point corresponds to the $\log_2$(Cy5/Cy3) signal for a single probe. Horizontal lines represent values expected for discrete number of copies in a diploid genome: blue line at 1, four copies; blue line at 0.585, three copies; thin black line at 0, two copies; and red line at −1, one copy. Approximate ORF locations are given beneath each plot. The region of *CUP1* amplification is shaded in purple. (D) As in A, sequencing results for *CDC11* amplified from a cold-insensitive derivative of C17.01D (Cs$^+$) passaged only in the cold and at room temperature, or passaged at 37° (post 37°). (E) Cells of C17.01D were grown at room temperature (~22°) to mid-log phase, fixed with ethanol, and stained with 4′,6-diamidino-2-phenylindole (DAPI). A grayscale fluorescent image was inverted and contrast adjusted to improve visibility. Arrowheads, distinct nuclear bodies. Bar, 5 μm.

clearly represented (Figure 2A), indicative of two alleles of *CDC11* in the same purportedly haploid strain (Moir *et al.* 1982). Two strains (C17.01D and N84.06D) had the same six mixed positions, of which only one was a coding change (G29D), and the other two strains (P44.08C and Q26.15D) had the same single mixed position, causing the coding change G32E. To confirm the presence of two *CDC11* alleles in C17.01D, we exploited a restriction site introduced by one of the silent mutations and digested a PCR product amplified from one such strain, yielding the expected pattern of one uncut species and one singly cut species (Figure S2A). Remarkably, the coding changes are identical to P-loop mutations we identified in Ts$^-$ *cdc11* mutants (Figure 1B, Table 1), yet the Cs$^-$ strains grew normally at 37° (Figure 2B).

We hypothesized that the two alleles arose from a local duplication of the *CDC11* locus and amplified and sequencing nearby genes to identify those without mixed peaks that would define the boundaries of the duplication. To our surprise, in addition to mixed peaks in the genes that flank *CDC11* on chromosome (Chr) X, *HOC1* and *MIR1*, we detected two alleles of *HAM1* (Figure S2B), ~7 kb away, suggesting the duplication might be large enough to alter the mobility of Chr X in pulsed-field gel electrophoresis (PFGE). This analysis revealed a range of apparent karyotypes in the Cs$^-$ mutants: some appeared normal, whereas strain N84.06D harbored at least one extra, missized copy of nearly every chromosome (Figure S2C).

Ultimately, we used array-CGH to quantify the copy number of nearly every protein-coding locus in the genome in the four *cdc11* Cs$^-$ strains. Relative to a reference strain (BY4741), *CDC11* (Figure 2C) and the vast majority of other loci were present at the same copy number, with a few anticipated exceptions: loci that in the reference strain harbored deletion alleles of auxotrophic markers (*ura3Δ0* and *lys2Δ0*) were overrepresented relative to the *URA3 LYS2* Cs$^-$ strains, and loci that frequently undergo spontaneous changes in copy number (*CUP1*, Ty1 transposable elements) were present at variable levels in some strains (Figure 2C and data not shown). For many of the former instances, the copy number ratio was ~0.5 relative to the rest of the genome (data not shown), demonstrating that, for each Cs$^-$ strain, most of the genome, including *CDC11*, is present at two copies per cell.

Two other copy number variations were observed in strain C17.01D. A portion of the *SAK1* gene was amplified (Figure S2D), and there was a segmental deletion between

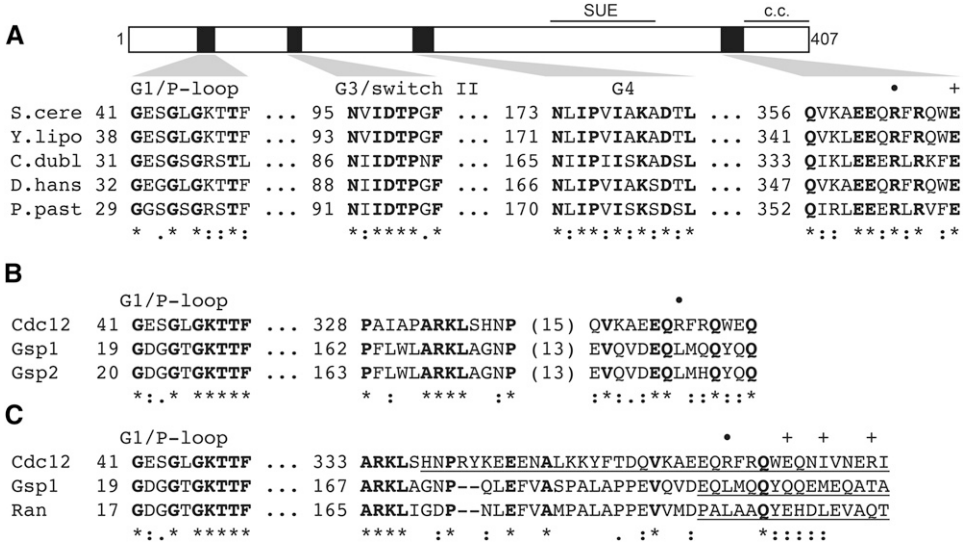

Figure 3 A conserved domain surrounding Cdc12 Arg 363 may allosterically regulate the G interface. ClustalW2 alignments of *S. cerevisiae* Cdc12 with Cdc12 homologs from other fungi, or other small GTPases. Above each group of sequences are labels of key GTPase motifs and other features of note: "•," Cdc12 Arg 363; "+," hydrophobic residues in Cdc12 matching the heptad repeat pattern consistent with coiled-coil-forming ability. Residues identical in all aligned sequences are in boldface type. Below each group of sequences, conservation is indicated by the following symbols: "*," positions with a single, fully conserved residue; ":," conservation between groups of strongly similar properties; and "." conservation between groups of weakly similar properties. (A) Top, to-scale graphical representation of Cdc12 domain/motif organization, with numbers indicating first and final residues of full-length Cdc12. "SUE," septin unique element (Versele and Thorner 2005). "c.c.," hydrophobic heptad repeats thought to form a coiled coil with those of Cdc3. Bottom alignments, "S.cere," *Saccharomyces cerevisiae* Cdc12; "Y.lipol," *Yarrowia lipolytica* YALI0D27148p; "C.dubl," *Candida dubliniensis* putative septin, GenBank accession no. CAX41392.1; "D.hans," *Debaromyces hansenii* DEHA2G12606p; "P.past," *Pichia pastoris* GenBank accession no. CAY71029.1. (B) The yeast Ran homologs Gsp1 and Gsp2 are most homologous to Cdc12 in their G1/P-loop motif, and in the region surrounding Cdc12 Arg 363. (C) The carboxy-terminal extensions of Cdc12 and Gsp1/Ran share predicted structural features in a region of Ran known to allosterically regulate conformations of protein–protein interaction interfaces. Underlined sequences have high alpha-helical propensity, based on jpred (http://www.compbio.dundee.ac.uk/www-jpred/index.html) and/or are known from crystal structures to be helical (Koyama and Matsuura 2010).

the *ALD3* and *ALD2* genes (data not shown). Sak1 is a member of the SNF1/AMPK family of protein kinases, whose other members in yeast are Tos3 and Elm1. Elm1 regulates septin function in poorly understood ways, likely by activating septin kinases (Asano *et al.* 2006). Elm1, Sak1, and Tos3 share overlapping function in the phosphorylation of Snf1 (Hong *et al.* 2003), but there is no evidence that Sak1 normally regulates septins. Thus, while amplification of a portion of the *SAK1* coding sequence might modify septin ring assembly dynamics, we doubt this event is biologically relevant, considering that the other three *cdc11* Cs$^-$ strains lack this amplification. Similarly, the *ALD2* and *ALD3* genes are 91% identical at the nucleotide level and arranged in a tandem fashion, suggesting that they originated from a gene duplication event that was simply reversed in strain C17.01D without phenotypic consequence.

With the exception of *cdc12(G247E)* (see below), all Ts$^-$ septin mutant alleles, including *cdc11(G29D)* and *cdc11 (G32E)*, are reportedly recessive for that phenotype (Hartwell *et al.* 1973; Casamayor and Snyder 2003; Nagaraj *et al.* 2008), but whether heterozygous diploid cells are generally Cs$^-$ was unknown. A BY4741-background *cdc11(G29D)/ CDC11* heterozygous diploid strain created by mating was indistinguishable in cellular morphology and growth rate from the wild-type control at 14°, 22°, 30°, and 37° (Figure 2B and data not shown). Introducing a *CDC11* plasmid (pSB1) into a haploid *cdc11(G29D)* or *cdc11(G32E)* strain also failed to generate any Cs$^-$ phenotype (data not shown).

This analysis pointed to a complex genetic situation in the Cs$^-$ *cdc11* strains that, in cold temperatures, allows the mutant protein to interfere with septin function despite the presence of wild-type *CDC11*. This condition appeared to be unstable, because many cold-insensitive derivatives spontaneously appeared when the Cs$^-$ strains were plated to 14° (data not shown). However, amplification and sequencing of *CDC11* from these derivatives generated the same mixed peaks at the same positions (Figure 2D). We suspected that cells carrying both alleles might spontaneously lose one or the other, in either case generating a monoallelic (*CDC11* or *cdc11*) clone capable of 14° growth. If this "sorting" process occurred after plating, the resulting colonies might each be a mix of the two clonal genotypes. To test this hypothesis, we passaged several "revertant" strains at 37°, which should eliminate Ts$^-$ *cdc11(G29D)* or *cdc11(G32E)* cells and thereby "purify" the population. Indeed, sequencing of the *CDC11* gene from one of these populations revealed that only the wild-type allele remained (Figure 2D). By contrast, passaging at 37° without prior selection at 14° failed to eliminate either allele (data not shown), confirming that the diallelic Cs$^-$ clones are not Ts$^-$ and that at high temperatures the mutant allele does not interfere with septin function. We conclude that the presence of two *CDC11* alleles—one wild type and one encoding a P-loop mutant—in the same cell is necessary but not sufficient to prevent septin function in the cold.

We realized that while our PFGE and array-CGH data demonstrate that the Cs$^-$ *cdc11* strains have two copies per clone of most genes, these need not reside in the same nucleus: heterokaryons (cells with genetically distinct haploid nuclei sharing the same cytoplasm) would also generate the experimental results we observed. Indeed, DAPI staining of DNA in the C17.01D Cs$^-$ strain and examination by light

and fluorescence microscopy revealed that even at the permissive temperature of 22°, most cells were linked together in branched chains of elongated cells with multiple nuclei per chain, similar to the terminal arrest phenotype at 14° (Figure 2E). Thus, C17.01D may grow as a kind of coenocytic mycelium, in which nuclei with distinct genotypes could conceivably propagate relatively independently. The high frequency of revertants and the efficient allele sorting we observed are consistent with the mitotic instability of heterokaryons generated using a karyogamy mutant (Conde and Fink 1976).

A cold-sensitive cdc12 mutant identifies an uncharacterized, highly conserved domain that may allosterically influence the G interface

In the Cs⁻ *cla10-1* strain K3538, we discovered the mutation Cdc12 R363K, a highly conservative substitution within a region—between the "septin unique element" (Versele and Thorner 2005) and the hydrophobic heptad repeats predicted to form coiled coils (Figure 3A)—to which no structure or function has yet been assigned. To confirm that the R363K mutation was responsible for the *cla10* and Cs⁻ phenotypes, we obtained two independent Cs⁺ derivatives of K3538. Each had reverted to Arg at position 363, become auxotrophic for adenine, and formed white colonies (data not shown), indicating that they were now *CLA10*, and able to tolerate the depletion of G1 cyclins caused by loss of the *ADE3 CLN3* plasmid (Cvrcková and Nasmyth 1993).

Among Cdc12 homologs in other fungal species, Arg 363 and the sequences immediately surrounding it are as highly conserved as the major GTPase motifs (Figure 3A). We further noticed that Gsp1 and Gsp2, paralogous relatives of the small GTPase Ran (Belhumeur *et al.* 1993), are the nonseptin *Saccharomyces cerevisiae* proteins with highest homology to Cdc12 (WU-BLAST2 $P = 0.0025$ and 0.0026, respectively), and that this homology is restricted to two motifs, the G1 box/P-loop and the portion of the Cdc12 C-terminal extension (CTE) that includes Arg 363 (Figure 3B). The homologous CTE in Ran (residues 173–216; Figure 3C) adopts distinct conformations in the GTP- and GDP-bound states (Vetter *et al.* 1999). Deletion of the CTE creates a constitutively active Ran by altering the conformations of the switch I and II regions of Ran(GDP) to mimic the GTP-bound state (Nilsson *et al.* 2002). If the corresponding region in the Cdc12 CTE acts in a similar way to allosterically modify conformations of the Cdc12 switch regions, then the restrictive temperature might "lock" the R363K mutant Cdc12 into a mimic of the GTP-bound state that is either incompatible with G heterodimerization or interacts with Cdc11 to render it unable to NC dimerize (see *Discussion*).

Cdc12(G247E) acts dominantly to interfere with septin function

Strikingly reminiscent of our results with the Cs⁻ *cdc11* mutants, we detected multiple alleles of *CDC12* in the moderately Ts⁻ and Cs⁻ strain K3538, one wild-type and one mutant

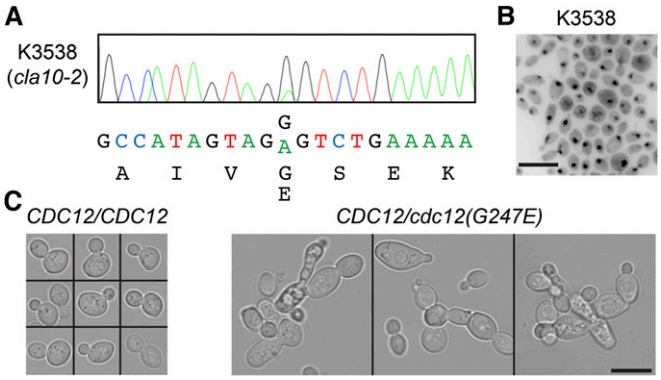

Figure 4 Cdc12(G247E) acts dominantly at high and low temperatures. (A) As in Figure 2A, dideoxy sequencing chromatogram demonstrating the presence of two nucleotides at a single position in a septin-encoding gene. Shown is a portion of *CDC12* amplified by PCR from genomic DNA of the Ts⁻ and Cs⁻ strain K3538. (B) As in Figure 2E, but for strain K3538. Bar, 5 μm. (C) Transmitted light images of diploid cells of the indicated genotypes in the BY4743 strain background grown to mid-log phase at 37°. Strains were *CDC12/CDC12*, BY4743 and *CDC12/cdc12(G247E)*, diploid made by mating BY4742 with CBY05110. Bar, 5 μm.

allele found previously in several Ts⁻ strains, *cdc12(G247E)* (Figure 4A, Table 1). Interestingly, this same mutation was first isolated (as *cdc12-1*) in the original *cdc* Ts⁻ screen by Hartwell *et al.* (1973) and is the only such mutant that was not strictly recessive, instead described as behaving in a semidominant manner in "some" (unidentified) strains. The steady-state level of total Cdc12 relative to the metabolic enzyme glucose-6-phosphate dehydrogenase (Zwf1) was at least twofold higher in the K3538 (*cla10-2*) strain than in the other three *cla10* strains (Figure S1B), suggesting that K3538 cells carry two copies of *CDC12* but one of most other genomic loci. Furthermore, K3538 cells cultivated at 30° appeared to be mononucleate (Figure 4B). We found that a heterozygous *cdc12(G247E)/CDC12* diploid strain of the BY4743 background created by crossing a *cdc12(G247E)* haploid with a wild-type haploid proliferated normally at 37° but exhibited a high proportion of cells (~25%) with morphological defects (Figure 4C). Thus, *cdc12(G247E)* is unique among the G interface mutations described here (Table 1) or elsewhere (Nagaraj *et al.* 2008) in its ability to interfere in mononucleate cells with septin function in the presence of a wild-type allele of the same septin.

Septin-subunit-specific effects on the thermostability of septin rings

Others have examined the defects of certain Ts⁻ septin mutants at high temperatures and found that GTP-binding-defective mutant cells were unable to assemble new rings, but preexisting rings were relatively stable (Dobbelaere *et al.* 2003; Nagaraj *et al.* 2008), consistent with bound GTP/GDP playing a structural role in new assembly that is less important in the thermal stability of the final product. We extended this analysis to unbiased mutants. S-phase arrest using HU allows rings assembled at low temperature to be tested for stability following a temperature upshift. Mutants clearly fell into two categories. Those in which

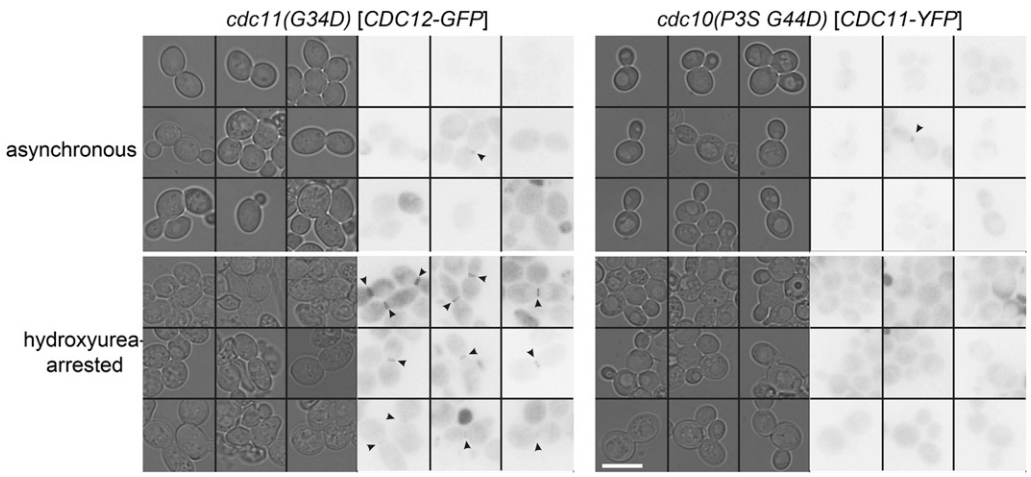

Figure 5 Defects in septin ring assembly and stability in temperature-sensitive septin mutants. Montages of representative brightfield (left) and fluorescence (right) micrographs of cells of the indicated genotype and carrying the indicated plasmid encoding a fluorescently tagged septin, following a shift from 23° to 37° for 120 min with or without a preceding HU-induced S-phase arrest. Arrowheads indicate extant septin rings. Strains and plasmids were *cdc10(P3S G44D)* [*CDC11-YFP*], CBY06424 with pML43 and *cdc11(G34D)* [*CDC12-GFP*], CBY06430 with pLP17. Grayscale fluorescence images were inverted and contrast adjusted to improve visibility. Bar, 5 μm.

rings disappeared from most cells in both conditions were classified as "stability" mutants, whereas those in which rings were absent in the majority of cells without HU but visible in HU-arrested cells were classified as "assembly" mutants. Representative images for particular mutants are shown in Figure 5, and results for the rest are summarized in Table 1.

The *cdc3(G365R)* and all five *cdc11* Ts⁻ mutants tested were determined to be assembly mutants (Figure 5, Table 1, and data not shown), suggesting that initial G dimerization by the mutant molecules is inhibited by elevated temperatures, but the presence of mutant Cdc3 or Cdc11 subunits within the filamentous ring does not render it particulary thermolabile. In addition to *cdc12(G247E)*, we tested a temperature degron-tagged version of Cdc12 encoded by *cdc12-td* (Li *et al.* 2011). As expected from others' results in a different strain background (Dobbelaere *et al.* 2003), *cdc12(G247E)* was an assembly mutant (data not shown). *cdc12-td* was a stability mutant (data not shown), indicating that even when incorporated into the ring, Cdc12 molecules can be extracted and degraded by the proteasome, leading to disassembly of the entire structure. Unexpected was the observation that all five *cdc10* mutants tested were stability mutants (Figure 5, Table 1, and data not shown), even those with identical substitutions in positions equivalent to *cdc11* assembly mutants [*e.g.*, Cdc10(G44D) and Cdc11(G34D), see Figure 1B]. These findings demonstrate that septin rings with mutant Cdc10 subunits are unstable at high temperature, in contrast with earlier studies in which a different, directed P-loop mutant of Cdc10 [*cdc10(G42V)*] mutant was deemed an assembly mutant (Nagaraj *et al.* 2008). However, after 90 min at 37° the fraction of HU-arrested *cdc10(G42V)* cells with rings was the lowest of any nucleotide-binding-pocket mutant tested in that study (Nagaraj *et al.* 2008). We held HU-arrested *cdc10* cells at 37° for 120 min, which likely allowed us greater sensitivity in detecting ring stability effects. Moreover, the *cdc10(G42V)* mutant was only mildly Ts⁻ (normal growth at 34°) (Nagaraj *et al.* 2008), whereas the *cdc10* mutants we examined grew poorly at 30° and above (data not shown), suggesting that the directed G42V substitution was less effective at inhibiting nucleotide binding than unbiased mutants selected on the basis of their temperature sensitivity. We consider it unlikely that a given substitution in the nucleotide-binding pocket has a more severe effect on nucleotide binding by Cdc10 than by Cdc11. Instead, we wondered whether the septin ring might be better able to tolerate mutant Cdc11 subunits because there is another septin, Shs1, able to bind nucleotide and occupy the same position as Cdc11 does in septin heterooctamers (Figure 1A), potentially providing a stabilizing effect. To test this hypothesis, we deleted *SHS1* in *cdc11(G34D)* cells and tested ring stability in the double-mutant cells. Indeed, septins rings, formed at low temperature in *cdc11(G34D) shs1*Δ cells, disappeared at 37° despite S-phase arrest with HU (Table 1).

G dimerization, not nucleotide binding, is required for new ring assembly and ring stability at high temperatures

Bound nucleotide provides additional points of contact between two septins across a G dimer interface. At the same time, a G dimer interface provides additional points of contact to stabilize nucleotide binding. We set out to determine whether bound nucleotide is essential at high temperatures for the assembly of complexes competent for new septin ring formation at high temperatures, or, alternatively, whether nucleotide merely promotes the formation of G heterodimers that are essential for higher-order assembly. Pringle *et al.* (1986) noted decades ago that the most common spontaneous suppressors of Ts⁻ mutations in Cdc10 are mutations in Cdc3, and vice versa. We

hypothesized that at high temperatures mutants of Cdc10 adopt conformations that are incompatible in association with wild-type Cdc3, but certain substitutions might render Cdc3 capable of "rescuing" the Cdc10 mutants by interacting with them, thereby bypassing the apparent requirement for nucleotide in high-temperature G heterodimerization.

The D182N substitution in Cdc10 that we identified in two independent *cdc10* Ts⁻ strains (Figure 1A, Table 1) very likely prevents GTP binding by Cdc10, as does the identical substitution in the corresponding position in human septin SEPT12 (Kuo *et al.* 2012). Cells of the *cdc10(D182N)* strain JPT193 were plated to 37° and a spontaneous suppressor of the Ts⁻ phenotype was isolated as a single colony after 3 days. The *CDC10* and *CDC3* coding regions were then amplified and sequenced. Consistent with our hypothesis, the original D182N mutation in *CDC10* persisted, and we found a single substitution in Cdc3, D210G, altering an absolutely conserved residue within the G3 loop/switch II region of the G dimer interface (Sirajuddin *et al.* 2009) (Figure 1B). Directed mutagenesis of Cdc3 Asp210 to Ala makes cells unable to grow at high temperature and grow slowly at moderate temperatures (Sirajuddin *et al.* 2009). In a *CDC10* background, *cdc3(D210G)* cells are not Ts⁻ but also have a minor growth defect at all temperatures (Figure 6A), representing a rare example of reciprocal suppression: two mutations that alone cause clear phenotypes are able to rescue each other and restore normal growth when combined in the same strain.

Importantly, *cdc3(D210G)* does not simply allow cells to assemble polymerization-competent heterooligomers without Cdc10, as does the substitution G261V (McMurray *et al.* 2011a), because GFP-tagged Cdc10(D182N) was efficiently incorporated into the filamentous septin ring in *cdc10(D182N) cdc3(D210G)* cells (Figure 6C). We further find it exceedingly unlikely that the *cdc3(D210G)* mutation restores the ability of Cdc10(D182N) to bind and hydrolyze GTP. Accordingly, because septin rings are thermostable in *cdc10(D182N) cdc3(D210G)* cells, the ring instability observed in *cdc10(D182N) CDC3* cells (Table 1) cannot be attributed to a structural requirement for GDP in the Cdc10 pocket. Instead, even when formed at low temperature, the Cdc3•GTP–Cdc10•empty G heterodimer and/or the Cdc10•empty–Cdc10•empty NC homodimer interfaces are probably unstable at high temperatures.

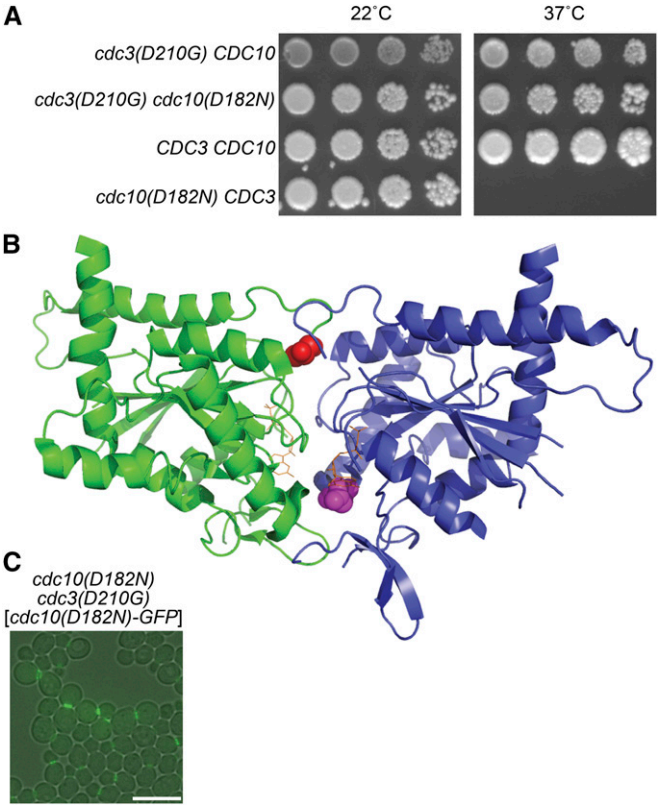

Figure 6 Mutation in the Cdc3 switch II region suppresses a G4 mutation in Cdc10. (A) Fivefold dilution series of cells of the indicated genotypes grown on YPD medium at the indicated temperatures for 2–3 days. Strains were *cdc3(D120G) CDC10*, MMY0131; *cdc3(D210G) cdc10(D182N)*, MMY0130; *CDC3 CDC10*, MMY0129; and *cdc10(D182N) CDC3*, MMY0128. (B) Structure of the SEPT2(GppNHp) G homodimer interface (PDB 3FTQ) with the residues corresponding to the sites of mutation in *cdc3(D210G) cdc10(D182N)* illustrated as colored spheres: red, Asp 201; magenta, Asp 185. (C) Cdc10(D182N)-GFP expressed from a low-copy plasmid in *cdc3(D210G) cdc10(D182N)* cells (strain MMY0110) grown to mid-log phase at 30° in YPD was visualized by epifluorescence microscopy (green) and overlaid on a transmitted light image. Bar, 5 μm.

Discussion

Assembly of septin heterooctamers in discrete, semiordered steps

Certain of the Ts⁻ mutants we analyzed were defective at high temperature specifically in the assembly of new rings. That rings in such assembly mutants are thermostable suggests that there is a discrete assembly step for which the act of nucleotide binding and/or G dimerization is important. Once this step has been accomplished, G dimers and all higher-order assemblies (octamers, filaments, rings) are stable. A compelling candidate for this step is NC homodimerization: mammalian septins that cannot G dimerize are unable to NC homodimerize *in vivo* (Kim *et al.* 2012), but NC homodimerization mutants form normal G dimers (McMurray *et al.* 2011a; Kim *et al.* 2012). *In vitro*, when the G interface of human SEPT2 is altered by preventing GTP hydrolysis, the NC interface adopts a nonnative conformation incompatible with homodimerization (Sirajuddin *et al.* 2009). Thus, perturbing GTP binding by the septins that form NC homodimers—as in *cdc10(G44D)* and *cdc11(G34D) shs1*Δ stability mutants (Table 1)—may destabilize septin assemblies because in the context of a G dimer formed at the permissive temperature, these mutant septins adopt quasinative conformations in which NC homodimers cannot tolerate subsequent shifts to high temperatures. By contrast, NC heterodimers appear not to require prior G dimerization at any temperature, because immunoprecipitation experiments at the restrictive

temperature in yeast cells carrying Ts⁻ alleles demonstrate that the Cdc3–Cdc12 NC heterodimer forms efficiently in *cdc10* mutants wherein the Cdc10–Cdc3 G dimer fails to assemble, and in *cdc11* or *cdc12* mutants wherein the Cdc11–Cdc12 G dimer fails to assemble (Nagaraj *et al.* 2008). This view predicts a semiordered assembly: nucleotide-facilitated formation of G heterodimers (Cdc3–Cdc10, Cdc11/Shs1–Cdc12) and nucleotide-independent Cdc3–Cdc12 NC heterodimerization occur simultaneously, followed by NC-homodimer-mediated joining of the resulting Cdc12–Cdc11–Cdc3–Cdc10 heterotetramers into heterooctamers and ultimately into filaments (Figure 7A).

Nucleotide binding promotes septin heterooligomerization via conformational changes in the subunit–subunit interfaces

The majority of the substitutions we discovered in Ts⁻ and Cs⁻ septin mutants insert bulky and/or highly charged sidechains (Arg, Asp, Glu, and Phe) in place of small, uncharged ones (Gly and Ser) whose equivalents in septins of known structure are in close proximity to bound nucleotide (Figure 1, B and C). Steric and/or electrostatic interference with occupancy of the pocket by GTP/GDP is likely the most important consequence of such mutations, rather than loss of individual contacts with bound nucleotide: a bulky, charged G3 box substitution (G100E) caused Ts⁻ growth in two *cdc10* strains (Figure 1, A and B), whereas in earlier studies substituting the equivalent Gly in Cdc11 or Cdc12 to Ala had no phenotypic effect (Nagaraj *et al.* 2008). However, it is difficult to determine exactly to what extent these mutations prevent GTP binding or hydrolysis *in vivo*, since appropriate biochemical experiments are challenging, if not impossible.

Structural modeling predicts that Cdc10(D182N) and Cdc12(G247E) should render the pocket entirely incompatible with a guanosine base (C. Musselman, unpublished observations), but bulky substitutions in the P-loop—where contacts with the phosphates are made—might only restrict binding to certain guanosine phosphoforms. In support of this idea, we found a strong synthetic genetic interaction between the P-loop mutant *cdc11(G29D)* and *cdc12(E188L)*, a directed mutation of a residue in Cdc12 predicted based on homology to human septins (Sirajuddin *et al.* 2009) to contact the guanosine base of the nucleotide bound in the pocket of Cdc11 (C. R. Johnson and M. A. McMurray, unpublished results). This Cdc12 mutation should have had little effect if the pocket of Cdc11(G29D) is nucleotide-free. Zent and Wittinghofer (2013) recently reported that human SEPT7 can bind nonphosphorylated guanosine, which favors a nonnative conformation of the G interface that is competent for assembly of a mixed dimer with SEPT7 bound to a nonhydrolyzable GTP analog (GppNHp). We speculate that at least some of the P-loop mutants of Cdc10 and Cdc11 bind guanosine or GMP *in vivo*, and the others prevent nucleotide binding altogether, in either case, biasing the mutant proteins toward nonnative conformations at high temperatures (Figure 7B).

Alternatively, considering that the chemical mutagens with which most of these mutant strains were created cause specific nucleobase alterations (*e.g.*, G→A by EMS), certain septin proteins could be predisposed to acquire Ts⁻ mutations if the codons representing critical residues are easily mutated to nonconservative amino acid substitutions (*e.g.*, GGA→AGA and Gly→Arg). However, the specificity of P-loop mutations for Cdc10 and Cdc11 does not reflect biased codon usage at the relevant positions, because *CDC3* and *CDC12* use equivalent or identical codons for these highly conserved residues (data not shown). Instead, the pockets of Cdc3 and Cdc12 are apparently better able to tolerate even drastic single-residue substitutions without making cells Ts⁻, consistent with others' observations using directed mutations of residues predicted to contact GTP [*e.g.*, Cdc3(K132E) (Nagaraj *et al.* 2008) or Cdc3(D128A) (Sirajuddin *et al.* 2009)].

Indeed, the only single mutations in the pockets of Cdc3 or Cdc12 that cause strong growth defects are a directed substitution intended to block GTP hydrolysis by Cdc12—T75A, which kills cells even at moderate temperatures (Sirajuddin *et al.* 2009)—and Cdc12 G247E, which we identified in three Ts⁻ strains (Figure 1B, Table 1). Interestingly, structural modeling suggests that the pocket of Cdc12 (G247E) could accommodate the pyrimidine triphosphate CTP (C. Musselman, unpublished observations). We propose that GTP binding *per se* by Cdc12 is not critical for its function *in vivo*. Instead, the Cdc12 pocket must not be occupied by a nucleoside triphosphate, *i.e.*, GTP or CTP. Specifically, in Cdc12•GTP the conformations of the switch regions are incompatible with G dimerization with Cdc11. Cdc12•CTP adopts at all temperatures quasinative conformations that are competent for G dimerization, but in this G dimer neither septin is normal, just as in the dimer with SEPT7•GppNHp the SEPT7•(guanosine) is nonnative (Zent and Wittinghofer 2013). Indeed, in this scenario the nucleotide state of wild-type Cdc11 may also be altered (Figure 7C). The manifestations of these abnormalities depend on temperature and whether wild-type Cdc12•GDP is also present: at moderate and low temperatures, Cdc11 in heterooctamers containing Cdc12•CTP is able to mediate filament polymerization via NC homodimerization, but at high temperatures its NC interface is unable to homodimerize. When heterooctamers containing Cdc12•GDP are also present, native Cdc11 can interact with the nonnative Cdc11 molecules in Cdc12•CTP-containing heterooctamers, but only at moderate temperatures: in the cold, the two forms of Cdc11 are incompatible (Figure 7C). This model explains the Ts⁻ phenotype of *cdc12(G247E)* cells and the Ts⁻ and Cs⁻ phenotypes of the *cdc12(G247E)/CDC12* strain K3538 (Table 1). Cold-induced NC interface incompatibility between native and nonnative Cdc11 molecules also explains the Cs⁻ phenotype of the four strains with one wild-type and one P-loop-mutant *CDC11* allele (Figure 7D).

This scenario is strikingly similar to the apparent cause of certain cases of male infertility in humans: either of two

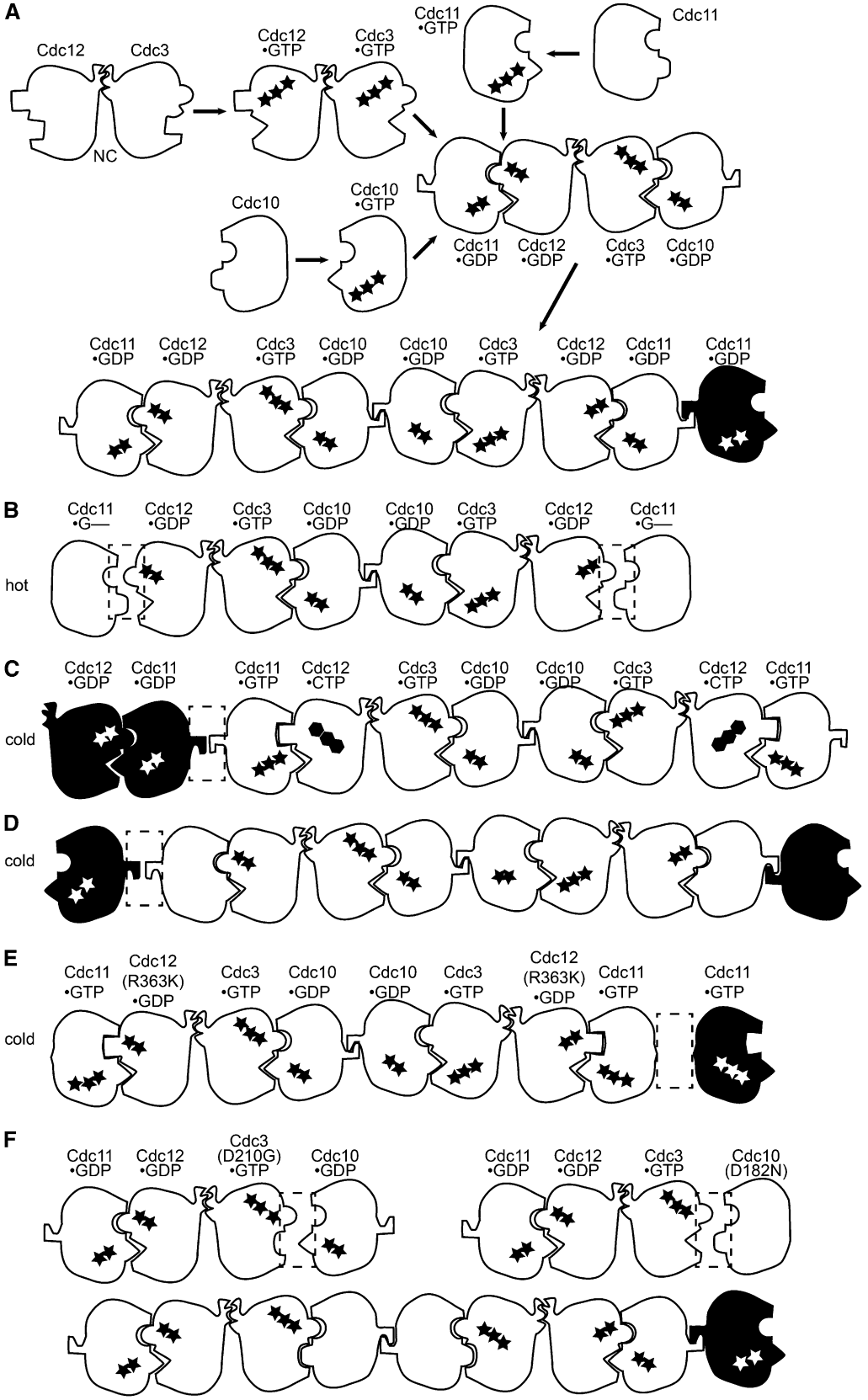

Figure 7 Models for conformational changes accompanying higher-order septin assembly and the effects of mutations and temperature. Nucleotide binding and hydrolysis states are speculative, as are the indicated conformational changes influencing septin–septin interactions. GTP is represented by three adjacent stars and GDP by two; CTP, three hexagons. G—, guanosine. Dashed box indicates incompatible/destabilized interface. (A) Stepwise assembly events in yeast septin heterooctamer assembly. (B) P-loop-mutant Cdc11 molecules bind unphosphorylated guanosine, favoring at high temperatures a conformation of the G interface unable to dimerize with Cdc12. (C) Cells expressing both *cdc12 (G247E)* and *CDC12*. Speculative effects on GTP hydrolysis by Cdc11 are included. (D) As in B, but in the cold and the presence of wild-type (GDP-bound) Cdc11. (E) *cdc12(R363K)* cells cultivated in the cold. (F) As illustrated, in *cdc3(D210G) CDC10*$^{+}$, *CDC3*$^{+}$ *cdc10(D182N)*, or *cdc3(D210G) cdc10(D182N)* cells cultivated at high temperatures.

GTP-binding-pocket mutations in SEPT12, the septin subunit thought to occupy, like Cdc11, the terminal position in testis-specific septin octamers (Figure 1A) acts dominantly to block assembly of the annulus (Kuo *et al.* 2012). The T89M substitution, which eliminates the Thr predicted to catalyze GTP hydrolysis (Sirajuddin *et al.* 2009), allows

SEPT12 to bind but not hydrolyze GTP (Kuo *et al.* 2012). SEPT12(D197N) prevents GTP binding altogether (Kuo *et al.* 2012) and is identical to the D182N substitution we identified in two *cdc10* Ts$^-$ strains (Figure 1, B and C, Table 1). Following the rationale of temperature-dependent NC interface incompatibility between heterooctamers with terminal subunits in distinct conformations, we can easily imagine how, once incorporated into heterooctamers, SEPT12•GTP and nucleotide-free SEPT12 could block annulus assembly by wild-type proteins during spermatogenesis in the testis, where the temperature is ~4° colder than the rest of the body. In a different GTP-binding protein, the α-subunit of the G protein-coupled receptor G_S, a mutation affecting a residue that also directly contacts bound nucleotide confers a testis-specific defect because the mutant protein is stable at 33° but degraded at 37°, suggestive of temperature-dependent conformational changes (Nakamoto *et al.* 1996). Similarly, the cold environment of the testis could lock the mutant septins into a filament-capping form.

Not all the Ts$^-$ and Cs$^-$ yeast mutations would be expected to cause defects in nucleotide binding *per se*. The *cdc12(R363K)* Cs$^-$ mutant altered a region of Cdc12 with homology to part of the GTPase Ran that controls the conformations of the switch regions (Nilsson *et al.* 2002). If in the cold Cdc12(R363K)•GDP mimics Cdc12•GTP, it could either destabilize the G interface with Cdc11 or induce in Cdc11 a conformation incompatible with NC homodimerization (Figure 7E). Additionally, one *cdc12* and all six *cdc3* Ts$^-$ strains harbored the same substitution in the same position (Cdc12 G268R; Cdc3 G365R), affecting a residue immediately adjacent to a Trp that makes a key G dimer contact outside the pocket (Sirajuddin *et al.* 2007; 2009; McMurray *et al.* 2011a; Kim *et al.* 2012) (Figure 1D). Phylogenetic analysis performed without structural knowledge identified this "Sep4" motif (WG) as being conserved in 92% of all septins (Pan *et al.* 2007). Among the other 8% is Cdc10, in which Ser (S256) is found instead of Gly (Figure 1C) and is the site of phosphorylation by the kinase Cla4 (Versele and Thorner 2004). Cla4 appears to promote septin ring assembly in parallel with nucleotide binding (Versele and Thorner 2004; Nagaraj *et al.* 2008), presumably by stabilizing septin–septin interactions like Cdc3–Cdc10. Thus, the substitutions to Arg we identified in the mutants could destabilize the Cdc3–Cdc10 or Cdc12–Cdc11 G interface at high temperatures while still allowing both protomers to interact normally with the nucleotides in their pockets.

Quality control of higher-order septin assembly: a "locals-only" competition?

Our models in which mutant septins act dominantly to interfere with septin function do not account for a "quality control" mechanism identified by others in which a wild-type septin "outcompetes" various nucleotide-binding-pocket mutant alleles for incorporation into septin rings at temperatures permissive for function of the mutants (Cid *et al.* 1998; Nagaraj *et al.* 2008). Cdc42 was proposed to preferentially recruit nucleotide-replete octamers to the site of septin ring assembly (Nagaraj *et al.* 2008). The dominance of Cdc12 (G247E) can be readily explained if binding to CTP is sufficient to pass quality control.

Why does quality control fail to prevent incorporation of the mutant Cdc11 and SEPT12 proteins in Cs$^-$ yeast and infertile men, respectively? Haploid spermatogonia express only one of the two parental septin alleles but share a common cytoplasm (Dym and Fawcett 1971). Septin mRNAs and/or proteins diffuse throughout, as evidenced by the facts that the annuli in *sept4* null sperm from a *SEPT4/sept4* heterozygous male are indistinguishable from their *SEPT4* counterparts (Ihara *et al.* 2005), and annuli were missing in all of the sperm from the *SEPT12(D182N)/SEPT12* man (Kuo *et al.* 2012). Perhaps quality control acts at the level of septin incorporation into octamers, rather than octamer incorporation into filaments, such that when newly translated septins are assembling into new octamers, nucleotide-bound subunits are preferentially incorporated at the expense of nucleotide-free mutant proteins. If a septin-encoding transcript does not diffuse far from its nucleus of origin prior to translation, then subsequent octamer assembly may occur locally, and a mutant, nucleotide-free protein translated near a mutant nucleus could evade quality control by incorporating into octamers at a subcellular location distinct from the site of assembly by wild-type octamers. Diffusion-based mixing of preassembled octamers within the shared cytoplasm would then allow mutant-containing octamers to interfere with ring assembly. This model would also explain the dominance of the mutant Cdc11 molecules in the putatively heterokaryonic *cdc11* Cs$^-$ yeast mutants.

Reciprocal genetic suppression identifies residues that dictate compatibility at the G interface

We propose that nucleotide-free Cdc10(D182N) is prone to adopting at high temperatures a conformation that, like Cdc10•GTP, is unable to associate with wild-type Cdc3•GTP, due in large part to steric and/or electrostatic interference by the charged sidechain of Cdc3 Asp210. Consistent with this idea, preventing GTP hydrolysis by Cdc10 via directed mutation renders cells Ts$^-$ (Sirajuddin *et al.* 2009). After we identified the *cdc3(D210G)* mutant, compelling biochemical support for this model was provided by analysis of purified human SEPT7, which is unable to form a SEPT7•GTP homodimer unless Asp103—homologous to Cdc3 Asp210, and which contacts Asp103 of the other protomer across the G interface of a SEPT7•GDP dimer (Zent *et al.* 2011)—is mutated to Ala (Zent and Wittinghofer 2013).

Loss of GTP binding by septins in evolution and disease

Intriguingly, a wild-type fission yeast septin, Spn7, has a drastically altered pocket lacking nearly all of the GTP-binding motifs, yet is capable of assembling efficiently into heterooctamers (Onishi *et al.* 2010). Spn7 occupies the same terminal position in septin octamers as does budding yeast Cdc11, but is expressed only during sporulation, when

septins form higher-order structures that are clearly distinct from the filamentous rings formed in mitosis (Onishi *et al.* 2010). Spn7 may have acquired the ability to adopt a G- and NC-dimerization-competent conformation without binding GTP, as we effectively reproduced in the lab with mutants of Cdc3 and Cdc10. Doing so would presumably sacrifice any ability to explore in a GTP-hydrolysis-coupled manner a wider range of stable conformations, but higher-order septin assembly in sporulating yeast may not require such regulated dynamics. Alternatively, Spn7 may have evolved to bind a non-GTP nucleotide; indeed, nucleotide pools undergo dramatic developmental remodeling during sporulation, at least in budding yeast (Jakubowski 1986; Jakubowski and Goldman 1988).

Considering that one of the infertility-causing septin mutations causes the same substitution as in Cdc10 (D182N), our findings clearly suggest that altering the G dimerization partner of SEPT12(D197N) by mutation or overexpression might rescue human septin function, and provide a general perspective for the development of therapeutic interventions targeted to disorders arising from septin mutations. Alternatively, it may be possible to slightly alter the temperature of an affected tissue/organ (*i.e.*, the testis) to bias the conformation of a mutant protein toward the native, functional form. From the opposite perspective, there may be no "permissive" temperature for higher-order septin assembly if more than one septin subunit is mutated, imposing multiple conformational constraints at distinct septin–septin interfaces within or between heterooligomers. Indeed, combining multiple Ts^- septin alleles in the same haploid yeast strain typically results in synthetic lethality (Longtine *et al.* 1996).

GTP binding and temperature sensitivity in cytoskeletal heteropolymers

It is particularly informative to compare our septin results to analysis of mutants of yeast α- and β-tubulin, the subunits of the heterodimer building block of microtubules. The substitutions in heat-sensitive tubulin mutants mapped almost exclusively to the α–β heterodimer interface, whereas cold-sensitive mutants harbored substitutions in residues that make contacts with other heterodimers in the context of a polymer (Richards *et al.* 2000). We propose that *de novo* assembly of the building blocks of septin or tubulin polymers requires the one-time acquisition of a single conformation, whereas the dynamic processes of polymerization and depolymerization require the polymerization interfaces to cycle through a set of discrete conformations. As with α-tubulin, which binds GTP but never hydrolyzes or exchanges it, nucleotide binding by septins plays a structural role in building block assembly, but for septins this role is only necessary in certain situations. High temperature makes it difficult for septins with no (or the wrong) nucleotide to adopt the conformation required to assemble the building blocks, and cold temperature constrains conformational flexibility, making it harder for the building blocks to come together into higher-order structures.

Acknowledgments

We are deeply indebted to John Pringle for providing unpublished yeast strains and detailed information about them and to Jeremy Thorner for essential support and insight. Catherine Musselman modeled the structures of key substitutions and predicted effects on nucleotide binding. Genome stability research in the Argueso laboratory is supported by American Cancer Society grant ACS IRG no. 57-001-53 and by an "Early Career Investigator" Webb-Waring Biomedical Research Award from the Boettcher Foundation to J.L.A. Work in the McMurray laboratory is supported by the National Institutes of Health (National Institute of General Medical Sciences R00 GM086603).

Literature Cited

Adams, A. E., and J. R. Pringle, 1984 Relationship of actin and tubulin distribution to bud growth in wild-type and morphogenetic-mutant *Saccharomyces cerevisiae*. J. Cell Biol. 98: 934–945.

Argueso, J. L., J. Westmoreland, P. A. Mieczkowski, M. Gawel, T. D. Petes *et al.*, 2008 Double-strand breaks associated with repetitive DNA can reshape the genome. Proc. Natl. Acad. Sci. USA 105: 11845–11850.

Asano, S., J.-E. Park, L.-R. Yu, M. Zhou, K. Sakchaisri *et al.*, 2006 Direct phosphorylation and activation of a Nim1-related kinase Gin4 by Elm1 in budding yeast. J. Biol. Chem. 281: 27090–27098.

Belhumeur, P., A. Lee, R. Tam, T. DiPaolo, N. Fortin *et al.*, 1993 *GSP1* and *GSP2*, genetic suppressors of the *prp20–1* mutant in *Saccharomyces cerevisiae*: GTP-binding proteins involved in the maintenance of nuclear organization. Mol. Cell. Biol. 13: 2152–2161.

Brachmann, C. B., A. Davies, G. J. Cost, E. Caputo, J. Li *et al.*, 1998 Designer deletion strains derived from *Saccharomyces cerevisiae* S288C: a useful set of strains and plasmids for PCR-mediated gene disruption and other applications. Yeast 14: 115–132.

Casamayor, A., and M. Snyder, 2003 Molecular dissection of a yeast septin: distinct domains are required for septin interaction, localization, and function. Mol. Cell. Biol. 23: 2762–2777.

Cid V. J., L. Adamíková, R. Cenamor, M. Molina, M. Sánchez *et al.*, 1998 Cell integrity and morphogenesis in a budding yeast septin mutant. Microbiology 144 (Pt 12): 3463–3474.

Conde, J., and G. R. Fink, 1976 A mutant of *Saccharomyces cerevisiae* defective for nuclear fusion. Proc. Natl. Acad. Sci. USA 73: 3651–3655.

Cvrcková, F., and K. Nasmyth, 1993 Yeast G1 cyclins CLN1 and CLN2 and a GAP-like protein have a role in bud formation. EMBO J. 12: 5277–5286.

Cvrcková, F., C. De Virgilio, E. Manser, J. R. Pringle, and K. Nasmyth, 1995 Ste20-like protein kinases are required for normal localization of cell growth and for cytokinesis in budding yeast. Genes Dev. 9: 1817–1830.

Dobbelaere, J., M. S. Gentry, R. L. Hallberg, and Y. Barral, 2003 Phosphorylation-dependent regulation of septin dynamics during the cell cycle. Dev. Cell 4: 345–357.

Dym, M., and D. W. Fawcett, 1971 Further observations on the numbers of spermatogonia, spermatocytes, and spermatids connected by intercellular bridges in the mammalian testis. Biol. Reprod. 4: 195–215.

Farkasovsky, M., P. Herter, B. Voss, and A. Wittinghofer, 2005 Nucleotide binding and filament assembly of recombinant yeast septin complexes. Biol. Chem. 386: 643–656.

García, G., A. Bertin, Z. Li, Y. Song, M. A. McMurray *et al.*, 2011 Subunit-dependent modulation of septin assembly: budding yeast septin Shs1 promotes ring and gauze formation. J. Cell Biol. 195: 993–1004.

Ghossoub, R., Q. Hu, M. Failler, M.-C. Rouyez, B. Spitzbarth *et al.*, 2013 Septins 2, 7 and 9 and MAP4 colocalize along the axoneme in the primary cilium and control ciliary length. J. Cell Sci. 126: 2583–2594.

Hartwell, L. H., 1971 Genetic control of the cell division cycle in yeast. IV. Genes controlling bud emergence and cytokinesis. Exp. Cell Res. 69: 265–276.

Hartwell, L. H., R. K. Mortimer, J. Culotti, and M. Culotti, 1973 Genetic control of the cell division cycle in yeast: V. Genetic analysis of *cdc* mutants. Genetics 74: 267–286.

Healy, A. M., S. Zolnierowicz, A. E. Stapleton, M. Goebl, A. A. DePaoli-Roach *et al.*, 1991 *CDC55*, a *Saccharomyces cerevisiae* gene involved in cellular morphogenesis: identification, characterization, and homology to the B subunit of mammalian type 2A protein phosphatase. Mol. Cell. Biol. 11: 5767–5780.

Hong, S.-P., F. C. Leiper, A. Woods, D. Carling, and M. Carlson, 2003 Activation of yeast Snf1 and mammalian AMP-activated protein kinase by upstream kinases. Proc. Natl. Acad. Sci. USA 100: 8839–8843.

Hu, J., X. Bai, J. R. Bowen, L. Dolat, F. Korobova *et al.*, 2012 Septin-driven coordination of actin and microtubule remodeling regulates the collateral branching of axons. Curr. Biol. 22: 1109–1115.

Ihara, M., A. Kinoshita, S. Yamada, H. Tanaka, A. Tanigaki *et al.*, 2005 Cortical organization by the septin cytoskeleton is essential for structural and mechanical integrity of mammalian spermatozoa. Dev. Cell 8: 343–352.

Jakubowski, H., 1986 Sporulation of the yeast *Saccharomyces cerevisiae* is accompanied by synthesis of adenosine 5-tetraphosphate and adenosine 5-pentaphosphate. Proc. Natl. Acad. Sci. USA 83: 2378–2382.

Jakubowski, H., and E. Goldman, 1988 Evidence for cooperation between cells during sporulation of the yeast *Saccharomyces cerevisiae*. Mol. Cell. Biol. 8: 5166–5178.

Kim, M. S., C. D. Froese, M. P. Estey, and W. S. Trimble, 2011 SEPT9 occupies the terminal positions in septin octamers and mediates polymerization-dependent functions in abscission. J. Cell Biol. 195: 815–826.

Kim, M. S., C. D. Froese, H. Xie, and W. S. Trimble, 2012 Uncovering principles that control septin-septin interactions. J. Biol. Chem. 287: 30406–30413.

Koyama, M., and Y. Matsuura, 2010 An allosteric mechanism to displace nuclear export cargo from CRM1 and RanGTP by RanBP1. EMBO J. 29: 2002–2013.

Kuhlenbäumer, G., M. C. Hannibal, E. Nelis, A. Schirmacher, N. Verpoorten *et al.*, 2005 Mutations in *SEPT9* cause hereditary neuralgic amyotrophy. Nat. Genet. 37: 1044–1046.

Kuo, Y.-C., Y.-H. Lin, H.-I. Chen, Y.-Y. Wang, Y.-W. Chiou *et al.*, 2012 mutations cause male infertility with defective sperm annulus. Hum. Mutat. 33: 710–719.

Li, Z., F. J. Vizeacoumar, S. Bahr, J. Li, J. Warringer *et al.*, 2011 Systematic exploration of essential yeast gene function with temperature-sensitive mutants. Nat. Biotechnol. 29: 361–367.

Lippincott, J., and R. Li, 1998 Sequential assembly of myosin II, an IQGAP-like protein, and filamentous actin to a ring structure involved in budding yeast cytokinesis. J. Cell Biol. 140: 355–366.

Longtine, M. S., D. J. DeMarini, M. L. Valencik, O. S. Al-Awar, H. Fares *et al.*, 1996 The septins: roles in cytokinesis and other processes. Curr. Opin. Cell Biol. 8: 106–119.

Lundblad, V., and K. Struhl, 2001 *Yeast*, John Wiley & Sons, Hoboken, NJ.

Macedo, J. N. A., N. F. Valadares, I. A. Marques, F. M. Ferreira, J. C. P. Damalio *et al.*, 2013 The structure and properties of septin 3: a possible missing link in septin filament formation. Biochem. J. 450: 95–105.

McMurray, M. A., A. Bertin, G. García, L. Lam, E. Nogales *et al.*, 2011a Septin filament formation is essential in budding yeast. Dev. Cell 20: 540–549.

McMurray, M. A., C. J. Stefan, M. Wemmer, G. Odorizzi, S. D. Emr *et al.*, 2011b Genetic interactions with mutations affecting septin assembly reveal ESCRT functions in budding yeast cytokinesis. Biol. Chem. 392: 699–712.

Mostowy, S., and P. Cossart, 2012 Septins: the fourth component of the cytoskeleton. Nat. Rev. Mol. Cell Biol. 13: 183–194.

Nagaraj, S., A. Rajendran, C. E. Jackson, and M. S. Longtine, 2008 Role of nucleotide binding in septin-septin interactions and septin localization in *Saccharomyces cerevisiae*. Mol. Cell. Biol. 28: 5120–5137.

Nakamoto, J. M., D. Zimmerman, E. A. Jones, K. Y. Loke, K. Siddiq *et al.*, 1996 Concurrent hormone resistance (pseudohypoparathyroidism type Ia) and hormone independence (testotoxicosis) caused by a unique mutation in the G alpha s gene. Biochem. Mol. Med. 58: 18–24.

Nilsson, J., K. Weis, and J. Kjems, 2002 The C-terminal extension of the small GTPase Ran is essential for defining the GDP-bound form. J. Mol. Biol. 318: 583–593.

Oh, Y., and E. Bi, 2011 Septin structure and function in yeast and beyond. Trends Cell Biol. 21: 141–148.

Onishi, M., T. Koga, A. Hirata, T. Nakamura, H. Asakawa *et al.*, 2010 Role of septins in the orientation of forespore membrane extension during sporulation in fission yeast. Mol. Cell. Biol. 30: 2057–2074.

Pan, F., R. L. Malmberg, and M. Momany, 2007 Analysis of septins across kingdoms reveals orthology and new motifs. BMC Evol. Biol. 7: 103.

Pringle, J. R., S. H. Lillie, A. E. M. Adams, C. W. Jacobs, B. K. Haarer et al., 1986 Cellular morphogenesis in the yeast cell cycle, pp. 47–80 in *Yeast Cell Biology,* edited by J. Hicks. Alan R. Liss, New York.

Richards, K. L., K. R. Anders, E. Nogales, K. Schwartz, K. H. Downing *et al.*, 2000 Structure-function relationships in yeast tubulins. Mol. Biol. Cell 11: 1887–1903.

Sellin, M. E., S. Stenmark, and M. Gullberg, 2012 Mammalian SEPT9 isoforms direct microtubule-dependent arrangements of septin core heteromers. Mol. Biol. Cell 23: 4242–4255.

Sirajuddin, M., M. Farkasovsky, F. Hauer, D. Kühlmann, I. G. Macara *et al.*, 2007 Structural insight into filament formation by mammalian septins. Nature 449: 311–315.

Sirajuddin, M., M. Farkasovsky, E. Zent, and A. Wittinghofer, 2009 GTP-induced conformational changes in septins and implications for function. Proc. Natl. Acad. Sci. USA 106: 16592–16597.

Versele, M., and J. Thorner, 2004 Septin collar formation in budding yeast requires GTP binding and direct phosphorylation by the PAK, Cla4. J. Cell Biol. 164: 701–715.

Versele, M., and J. Thorner, 2005 Some assembly required: yeast septins provide the instruction manual. Trends Cell Biol. 15: 414–424.

Versele, M., B. Gullbrand, M. J. Shulewitz, V. J. Cid, S. Bahmanyar *et al.*, 2004 Protein-protein interactions governing septin heteropentamer assembly and septin filament organization in *Saccharomyces cerevisiae*. Mol. Biol. Cell 15: 4568–4583.

Vetter, I. R., C. Nowak, T. Nishimoto, J. Kuhlmann, and A. Wittinghofer, 1999 Structure of a Ran-binding domain complexed with Ran bound to a GTP analogue: implications for nuclear transport. Nature 398: 39–46.

Vrabioiu, A. M., S. A. Gerber, S. P. Gygi, C. M. Field, and T. J. Mitchison, 2004 The majority of the *Saccharomyces cerevisiae* septin complexes do not exchange guanine nucleotides. J. Biol. Chem. 279: 3111–3118.

Wach, A., A. Brachat, R. Poehlmann, and P. Philippsen, 1994 New heterologous modules for classical or PCR-based gene disruptions in *Saccharomyces cerevisiae*. Yeast 10: 1793–1808.

Winzeler, E. A., D. D. Shoemaker, A. Astromoff, H. Liang, K. Anderson *et al.*, 1999 Functional characterization of the *S. cerevisiae* genome by gene deletion and parallel analysis. Science 285: 901–906.

Zent, E., I. Vetter, and A. Wittinghofer, 2011 Structural and biochemical properties of Sept7, a unique septin required for filament formation. Biol. Chem. 392: 791–797.

Zent, E., and A. Wittinghofer, 2013 Human septin isoforms and the GDP-GTP cycle. Biol. Chem. .10.1515/hsz-2013–0268

Communicating editor: D. Lew

GENETICS

Supporting Information
http://www.genetics.org/lookup/suppl/doi:10.1534/genetics.114.161182/-/DC1

Higher-Order Septin Assembly Is Driven by GTP-Promoted Conformational Changes: Evidence From Unbiased Mutational Analysis in *Saccharomyces cerevisiae*

Andrew D. Weems, Courtney R. Johnson, Juan Lucas Argueso, and Michael A. McMurray

DOI: 10.1534/genetics.114.161182

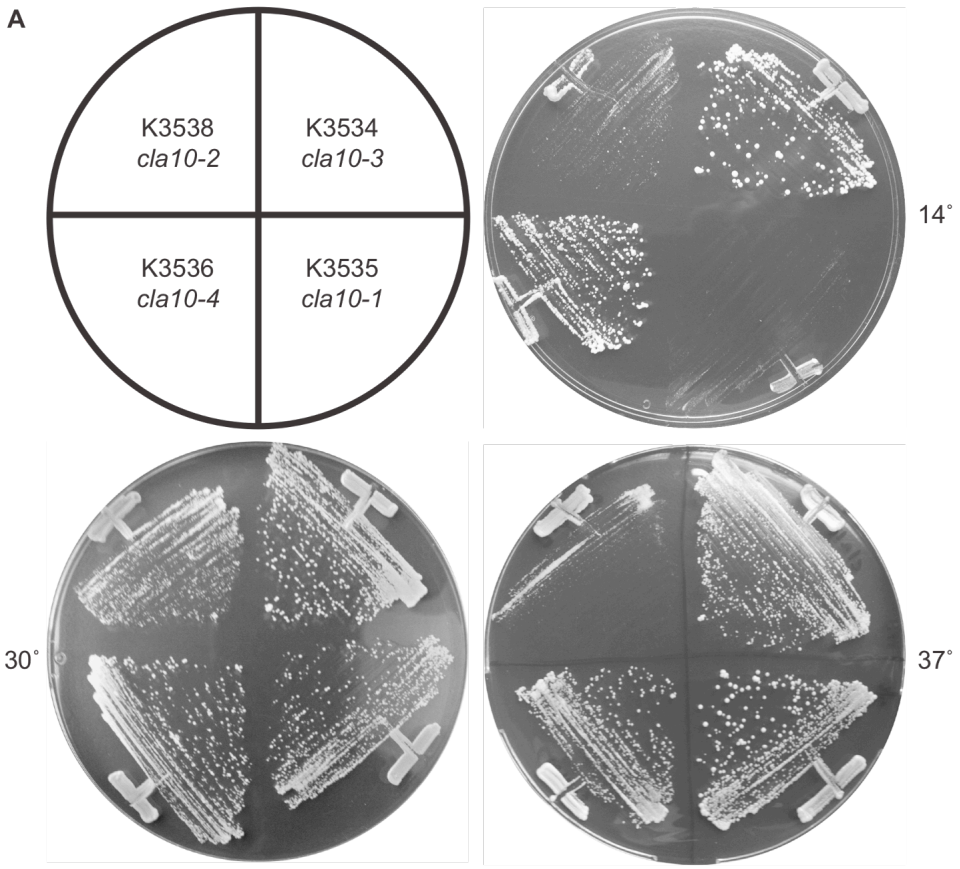

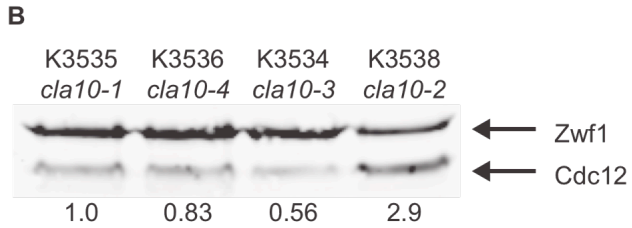

Figure S1 Heat- and cold-sensitive phenotypes and Cdc12 protein abundance in *cla10* mutants.
(A) The *cla10* strains K3534, K3535, K3536, and K3538 were streaked to YPD and cultivated at the indicated temperature.
(B) Total protein was extracted from the cells in (A) grown at 30˚, resolved on a 10% SDS-PAGE gel, and transferred to a polyvinylidene membrane, prior to exposure to rabbit anti-Cdc12 (Versele and Thorner 2004) and anti-Zwf1 (Sigma-Aldrich A9521) antibodies, consecutively. Fluorescent anti-rabbit secondary antibodies were used for detection. The background-corrected relative ratios of Cdc12 (47 kDa) to the loading control Zwf1 (58 kDa) were normalized to that of the *cla10-1* strain and are indicated below each lane.

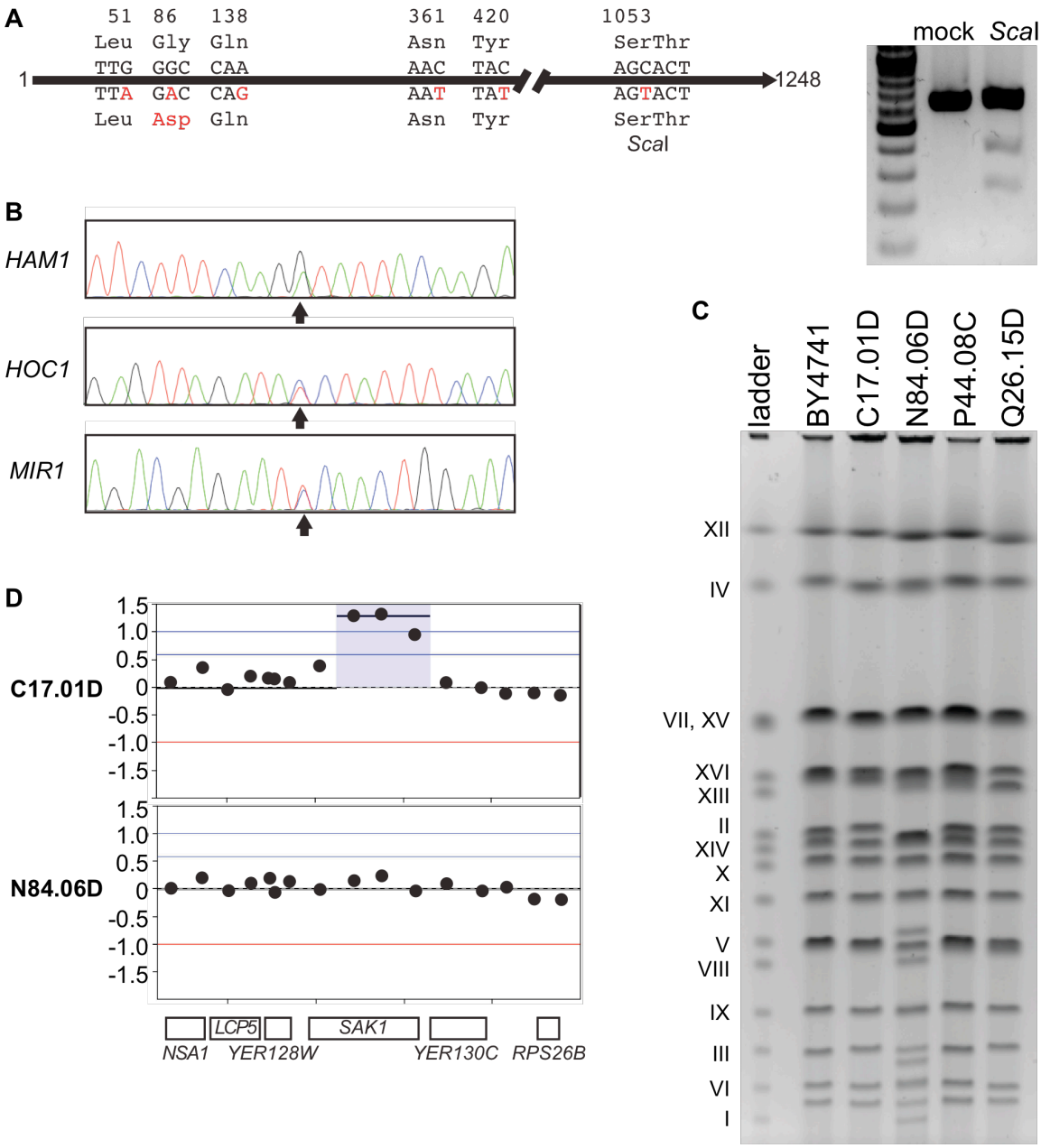

Figure S2 Cold-sensitive *cdc11* mutants carry two copies of the genome.
(A) Left, a schematic representation of the *CDC11* ORF indicating positions (in nucleotides) of mutations (red) found in strains N84.06D, and the amino acids encoded by affected codons. Sequences of the wild-type allele are given above, mutant sequences below. Below position 1053, a *Sca*I recognition site is present in the mutant alllele. Right, a PCR product encompassing the 3'-most ~620 nucleotides of the ORF plus ~30 nt of 3' sequence was incubated for 6 hr in buffer alone ("mock") or digested with *Sca*I, and resolved adjacent to a DNA ladder (GeneRuler DNA Ladder Mix, Thermo Scientific #SM0331) on a 1% sodium borate agarose gel containing ethidium bromide.
(B) As in Figure 2A, sequencing results from PCR products of the indicated genes flanking or nearby *CDC11* in strain N84.06D. Arrows indicate positions with multiple signals.
(C) PFGE of chromosomes isolated from the indicated strains, run adjacent to a ladder of *S. cerevisiae* chromosomes (Bio-Rad #170-3605). Labels on the left identify each chromosome in the ladder.
(D) As in Figure 4C, Array-CGH of copy number variation in strains C17.01D and N84.06D compared to BY4741. The extra black horizontal line in C17.01D corresponds to the average signal for probes in the region of SAK1 amplification, shaded in purple.